

# Simulation-Based Evaluation of Dense Convolutional Neural Networks for Skin Cancer Detection

Kavita Behara<sup>1</sup>, Ernest Bhero<sup>2</sup>, John Terhile Agee<sup>3</sup>

<sup>1</sup>Mangosuthu University of Technology, Durban, South Africa

<sup>2,3</sup>University of KwaZulu-Natal, 4041, South Africa

---

## Article Info

### Article history:

Received Aug 16, 2024

Revised Jan 11, 2025

Accepted Feb 5, 2025

---

### Keywords:

Deep learning

Machine learning

Medical diagnostics

Augmentation

Segmentation

---

## ABSTRACT

Skin cancer, particularly melanoma, poses significant challenges to public health, with early detection being critical for effective treatment. Traditional diagnostic methods often fall short, particularly in resource-limited settings. In response, artificial intelligence (AI) techniques, especially deep learning models, have emerged as promising tools for automated skin cancer detection. This study evaluates the performance of Dense Convolutional Neural Networks (DCNNs) in classifying and detecting skin lesions, leveraging simulation-based approaches to assess the effectiveness of various AI models. Utilizing datasets such as HAM10000 and ISIC2017, which contain a wide variety of skin types and lesion stages, the models were trained and tested using key performance metrics such as accuracy, precision, recall, and F1-score. The results show that DCNNs outperformed traditional machine learning techniques like Support Vector Machines (SVM), K-Nearest Neighbors (KNN), and Decision Trees (DT), demonstrating superior accuracy, generalization ability, and efficiency in handling large, imbalanced datasets. The simulation-based approach provided insights into the ability of DCNN models to manage dataset inconsistencies and class imbalances, showcasing their potential as robust tools for skin cancer detection. These findings highlight the ability of AI in advancing dermatological diagnostics, offering more timely and accurate detection, and potentially improving patient outcomes.

Copyright © 2025 Institute of Advanced Engineering and Science.  
All rights reserved.

---

## Corresponding Author:

Kavita Behara,

Department of Electrical Engineering,

Mangosuthu University of Technology, Durban, South Africa.

Email: beharak@mut.ac.za

---

## 1. INTRODUCTION

Skin lesions are phenotypic manifestations of skin cancer, representing abnormal variations in skin tissue. Skin cancer occurs when abnormal skin cells proliferate, often triggered by overexposure to ultraviolet (UV) radiation, leading to the abnormal growth of melanocytic cells on the skin [1], [2]. South Africa, due to its geographical location, experiences some of the highest levels of UV radiation globally and has the second-highest incidence rate of skin cancer, primarily melanoma, following Australia [3]–[5]. Melanoma is one of the deadliest forms of skin cancer and can be fatal if not detected early [6].

Healthcare systems worldwide, particularly in developing countries, are lagging in adopting advanced automated systems such as computer vision and AI. This delay exacerbates the strain on the healthcare sector, which faces significant shortages in medical diagnostic resources and undertrained health professionals for using advanced medical equipment [7], [8]. Many patients live in rural areas with limited access to healthcare experts and infrastructure [9], [10]. Consequently, clinicians rely heavily on manual diagnostic methods to screen and detect skin cancer, including visual inspection, clinical screening, dermoscopy analysis, biopsy, and histopathological examination [11], [12]. Also, Clinicians' inability to recognize early cancer invasion complicates accurate classification and makes it difficult to assess the extent of cancer invasion in the early stages. [13].

The rising incidence of skin cancer and the limitations of traditional diagnostic methods necessitate innovative and precise solutions. Conventional methods often struggle to detect the subtle early signs of cancer invasion, complicating accurate classification. This challenge is particularly pronounced when handling complex, large, and unbalanced datasets such as HAM10000, ISIC 2017, and PH2. As a result, manual detection methods are prone to errors, leading to delayed diagnoses and suboptimal patient outcomes [13].

The demand for non-invasive diagnostic techniques has increased in response to these challenges. These techniques include photography, dermoscopy, sonography, confocal microscopy, Raman spectroscopy, fluorescence spectroscopy, terahertz spectroscopy, optical coherence tomography, multispectral imaging, thermography, electrical bio-impedance, tape stripping, and computer-aided analysis [14]. Dermoscopy, an epiluminescence light microscopy that magnifies skin lesions, is one of the most common techniques for diagnosing skin cancer. Standard diagnostic methods include the ABCDE rule, pattern analysis, Menzies method, and the 7-Point Checklist [15].

Recent research shows AI has been at the forefront of diagnosing and classifying skin disorders such as skin cancer, psoriasis, and inflammatory diseases. Significant research has focused on using AI-based applications like computer vision, image processing, machine learning, and deep learning to identify and classify skin lesions, improving diagnostic accuracy and speed. Image classification, a critical task in medical imaging, involves standard steps such as image acquisition, preprocessing, segmentation, feature extraction, and classification. The effectiveness of classification algorithms heavily depends on feature sets, including shape, color, edges, and regions of interest [16]. Recent advancements in deep learning (DL) algorithms, in particular convolutional neural networks (CNNs), have shown enhanced and precise results, aiding quicker and more accurate diagnoses [17], [18]. Researchers have developed lightweight models for lesion self-diagnosis on smartphones [19], two-staged DL [20] techniques for automated melanoma localization, and segmentation networks like FC-dual-path network (FC-DPN) [21] to improve accuracy. Pixel-wise classification strategies and combinations of traditional and modern techniques have also been explored [22]. The author in [23] used fully convolutional networks (FCNs) with the VGG16 architecture and hand-crafted text-based features for melanoma lesion segmentation. While effective, it struggles with complex geometries and consistent visual appearances. ResNet-based approaches [24] and advanced object recognition frameworks like Faster-RCNN and fuzzy k-means clustering have achieved high accuracy but require substantial computational resources [25], [26]. Multiclass classification architectures [27] and deep learning frameworks such as YOLO [28] have further advanced the field. Another innovative approach is presented by Riyadi et al., who leveraged the YOLOv8n model for skin cancer detection and classification. YOLOv8n, a state-of-the-art deep learning model, has demonstrated significant improvements in both accuracy and real-time processing speed compared to traditional methods. The study highlights that YOLOv8n achieved an impressive accuracy of over 94% in classifying various skin lesion types, including melanoma and benign lesions [29]. In addition to YOLOv8n, other AI-driven solutions like DermAI was proposed by author of [30]. DermAI, an AI chatbot for dermatological diagnosis, achieved a 92% classification accuracy in diagnosing common skin diseases. Its user-friendly interface allows patients to receive quick diagnostic feedback, streamlining the process for both patients and clinicians [30].

Additionally, methods combining Mask RCNN and DenseNet201 [31], connected block LCNet DCNN models [32], and feature fusion techniques have been proposed, each with unique strengths and limitations. Ensemble machine learning techniques and novel data augmentation methods like SMOTE have also contributed to the field [33]. In [34], the authors developed an energy-saving service offloading system using deep reinforcement learning for low-cost healthcare monitoring, but it overburdens the system with additional energy consumption. In [35], a Smart Healthcare System for Severity Prediction and Critical Tasks Management (SHSSP-CTM) of COVID-19 Patients in IoT-Fog Computing Environments a Smart Healthcare System for COVID-19 severity prediction using Logistic Regression and Random Forest was developed. Despite these advancements, challenges remain with energy consumption, computational overhead, and handling different-sized lesions [35]. This comprehensive analysis of state-of-the-art methods highlights the ongoing efforts to enhance skin lesion classification and the need for further improvements to address existing limitations. Furthermore, a systematic review conducted by Furriel et al., explored various AI models for skin cancer detection and classification within clinical environments. The review compiled results from numerous studies, revealing that AI models, particularly deep learning algorithms, can reach diagnostic accuracy levels comparable to expert dermatologists. These findings suggest that AI models can significantly assist in early-stage diagnosis and reduce diagnostic errors. However, the review also emphasized the importance of further validation to ensure these models' safety, efficacy, and ethical application before they are fully adopted into clinical practices. As these technologies continue to evolve, their integration into clinical workflows could revolutionize dermatological practice by enabling faster, more reliable diagnoses and improving patient outcomes [36]. Appendix A analyses the state-of-the-art methods currently used for skin lesion classification.

The potential of AI to revolutionize skin cancer diagnostics is undeniable. Yet, significant gaps remain in the thorough, systematic evaluation of various AI techniques in real-world settings. Many existing AI models have not fully explored the direct application of AI to raw dermatological images for predicting outcomes, often relying heavily on clinician interpretation. Furthermore, generalization and interpretability persist, limiting the practical utility of these models. Models trained on specific datasets may not perform well across different populations, and the opaque nature of AI decisions can hinder clinical adoption. Although deep learning models have been extensively studied for automatic skin lesion categorization, their performance in actual medical settings still needs improvement. Critical issues that Alli et al. [33] raised in their application of deep learning models for the classification of skin lesions included:

- Large datasets are needed to train deep learning models to create more accurate automated clinical systems.
- Lack of real-time patient or hospital databases due to privacy concerns.
- Problems with class imbalance, duplicates, various dimensions, etc., exist in publicly accessible datasets.
- Another major hurdle in clinical applications is the cost of computational complexity and implementation time.

To address these challenges, the authors conducted simulation-based studies using various AI models, such as DCNN, SVM, KNN and Decision Trees, to assess and evaluate their performance on skin cancer datasets regarding accuracy, generalizability, and interpretability. This simulation study aims to identify more effective solutions that reduce errors and time constraints. By enhancing diagnostic accuracy and improving the generalizability and interpretability of AI models, we seek to empower dermatologists, expedite the diagnostic process, and ultimately improve patient outcomes. The main objective of this study is summarized as follows:

- Develop and simulate AI-based models that can classify skin lesions and use color, illumination, and resolution to identify melanoma skin cancer.
- Test the model's performance on a sizable dataset of images of skin lesions, balance the data and allow for efficient computation while improving the prediction accuracy. Utilize data and model generalisation techniques to distribute the skin lesion classes.
- Evaluate and compare the results of AI models, demonstrating their efficacy and improvements by assessing their accuracy, precision, recall and F1-Score in classifying and detecting skin cancer.

Figure 1 illustrates the schematic workflow of our simulated AI modelling used for skin cancer classification. The remaining sections of this manuscript are organized as follows: Section 2 presents the details of the simulation-based models, followed by respective discussions on the performance of the simulated results in Section 3. The detailed analysis of the simulation results of various AI models are covered in Section 4, and Section 5 contains the conclusion and future research directions.

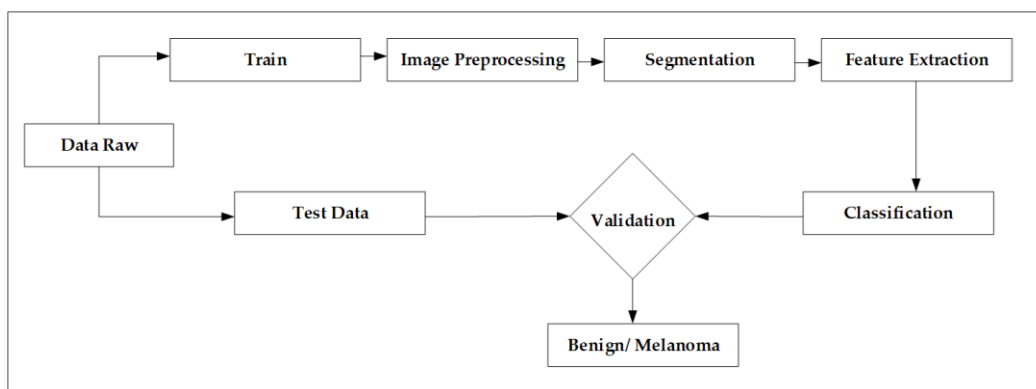


Figure 1. Schematic workflow for skin cancer classification

## 2. MATERIALS AND METHODS

### 2.1 Data Acquisition

Acquiring raw data from diverse image modalities is critical in image processing. This process may entail manually collecting data from hospitals and patients or utilizing publicly accessible web datasets. The quality of the input data significantly influences the efficiency and precision of disease detection. Notably, many dermoscopic datasets are freely accessible through open databases. The classification of standard datasets according to skin class is presented in Table 1.

Cassidy et al. [34] found that ISIC datasets are mainly used for binary classification and segmentation. Smaller datasets often reduce classification accuracy, and repeated images inflate dataset size. Removing duplicates is recommended to improve accuracy and reduce computation time [46]. Larger datasets enhance deep learning model performance. We trained the AI-based model on HAM10000 and ISIC 2017 datasets to diagnose skin lesions. The following sections detail the data preprocessing steps.

Table 1. The classification of standard datasets according to skin class

Dataset	Number of classes	Number of Images	Usage
ISIC 2020 [37]	8	33,126	Binary Classification
ISIC 2018 [38]	7	~10000	Binary Classification
HAM10000 [38]	7	10015	Multiclass Classification
ISIC 2017 [39]	3	~2000	Binary Classification
DermQuest [40]	2	~200	Binary Classification
MED-NODE [41]	2	~200	Binary Classification
PH2 [42]	3	~400	Binary Classification
ISBI 2016 [43]	2	~1200	Binary Classification
ISIC 2019 [44]	8	25331	Binary Classification

## 2.2 Exploratory Data Analysis

The limited quantity and lack of variety of dermatoscopic image datasets make it challenging to train neural networks for automated diagnosis of pigmented skin lesions [34]. We collected dermatoscopic images from various populations obtained and saved using multiple modalities. The HAM10000 dataset includes 10,015 dermatoscopic images and a CSV file with demographic data for each lesion, featuring seven skin lesion types: Actinic Keratosis (AKIEC) - 327, Dermatofibroma (DF) - 115, Benign Keratosis (BKL) - 1099, Melanoma (MEL) - 1113, Melanocytic nevi (NV) - 6705, Vascular Skin Lesion (VASC) - 142, and Basal Cell Carcinoma (BCC) - 514. The ISIC 2017 dataset contains 2000 dermatoscopic images and a CSV file with demographic data, including three skin lesion types: Benign nevi - 1372, Melanoma (MEL) - 374, and Seborrheic Keratosis - 254. Figure 2 illustrates the distribution of various skin lesion types within these two datasets.

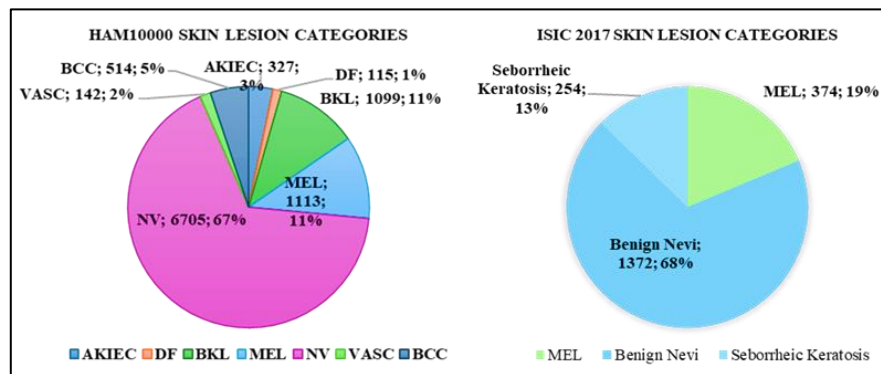


Figure 2. Frequency of raw data on skin lesion Types

Compared to human experts and used for machine learning, this benchmark dataset covers all major pigmented lesion diagnostic subtypes, with over 50% pathology-confirmed lesions. The rest are verified by follow-up, expert consensus, or in-vivo confocal microscopy, as depicted in Figure 3. We have also summarized the primary feature set, noting any anomalies and biases in the data.

The description of each skin lesion is detailed in Table 2, and Figure 4 shows the samples of each skin lesion category with 600x450 pixel resolution. Figure 5 shows that the lower extremity, back, and trunk are heavily affected skin cancer regions, and most patients exist between the ages of 40 and 60, as shown in Figure 6. The dataset also records that most occurrences of skin lesions are found in men, as depicted in Figure 7.

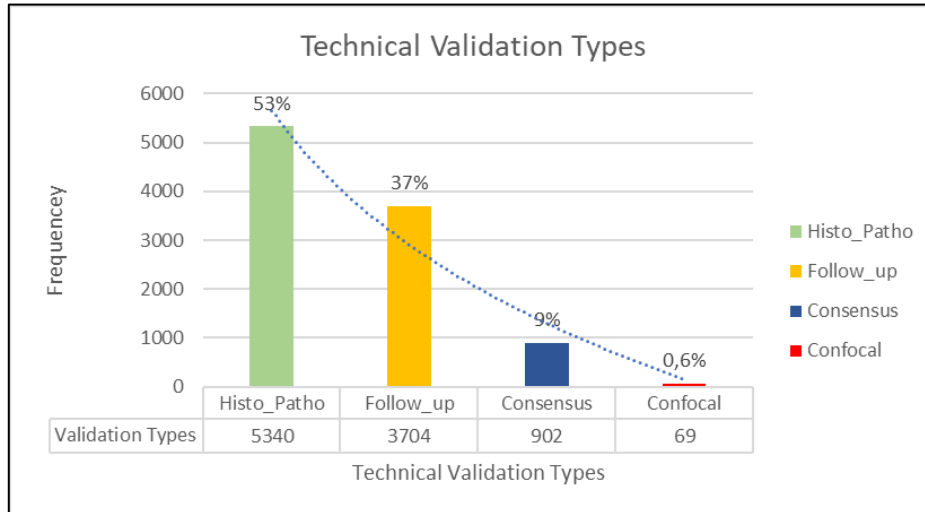


Figure 3. Distributions of the four different technical validation types

Table 2. Description of Skin Lesion Categories for HAM10000 and ISIC 2017

Skin Lesion Categories	Description	% Samples HAM10000	% Samples ISIC 2017
Actinic Keratosis and Intraepithelial Carcinoma/Bowen's Disease (ACKIEC)	It is the primary stage of SCC (Squamous Cell Carcinoma). It is a non-invasive variant and requires non-surgical treatment. AKIEC commonly appears on the face, whereas Bowen's Disease occurs in other locations on the body.	3	
Dermatofibroma (DF)	It is a benign skin lesion that appears brown with a central zone of fibrosis dermatoscopically; it occurs due to an inflammatory reaction to minimal trauma.	1	
Benign Keratosis-Like Lesions (BKL)	It includes three sub-classes: seborrheic keratosis, solar lentigo, and lichen-planus-like keratosis, which differ dermatoscopically but are similar histopathologically.	11	
Melanoma (MEL)	It is a malignant neoplasm of melanocytes that appears in different variants. Melanoma appears on various sites of the body and is the most dangerous malignant if it is not treated at an early stage.	11	19
Melanocytic Nevi (NV)	Appears as numerous variants and are benign neoplasms of melanocytes. Variants differ from the dermatoscopic point of view.	67	
Vascular Skin Lesion (VASC)	It appears as flat pink areas of discolouration and ranges to deep purple over time. It is related to the overgrowth of soft tissues and underlying bones, which develops a cobblestone effect on the skin over time.	2	
Basal Cell Carcinoma ()	It appears in different morphologic variants, including flat, nodular, pigmented, and cystic. It is an epithelial skin cancer variant less dangerous than other skin lesions but grows uncontrollably if untreated.	5	
Benign Nevi (BN)	A skin ailment known as a benign melanocytic nevus is distinguished by well-circumscribed, pigmented, round or oval lesions that are typically 2 to 6 mm in diameter. A benign melanocytic nevus can have pigmentation or hair as well.		68
Seborrheic Keratosis (SK)	A benign skin ailment manifests as a waxy brown, black, or tan growth—one of the most prevalent non-cancerous skin growths in elderly persons. The face, chest, shoulders, and back are typical for developing seborrheic keratoses. It looks somewhat raised, waxy, and scaly.		13

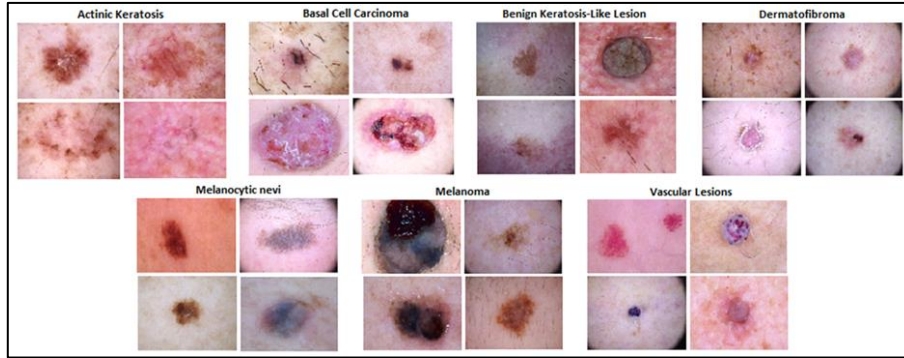


Figure 4. Sample Images of Training Dataset

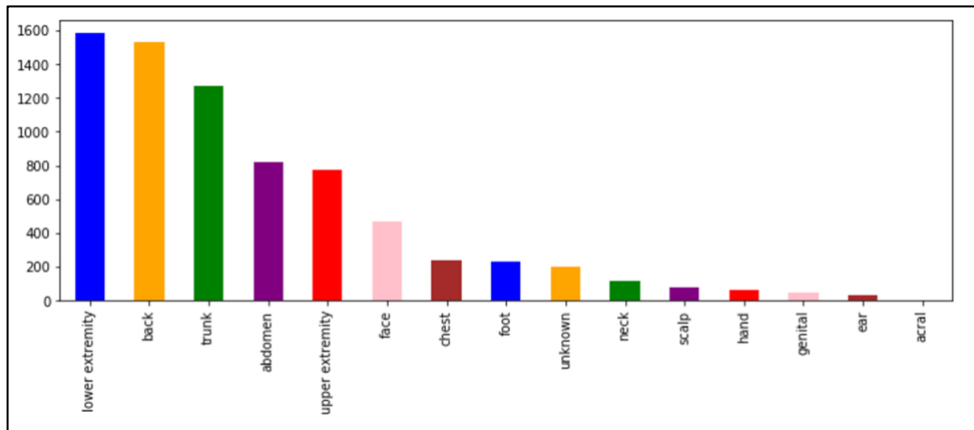


Figure 5. Distribution of location of skin lesions

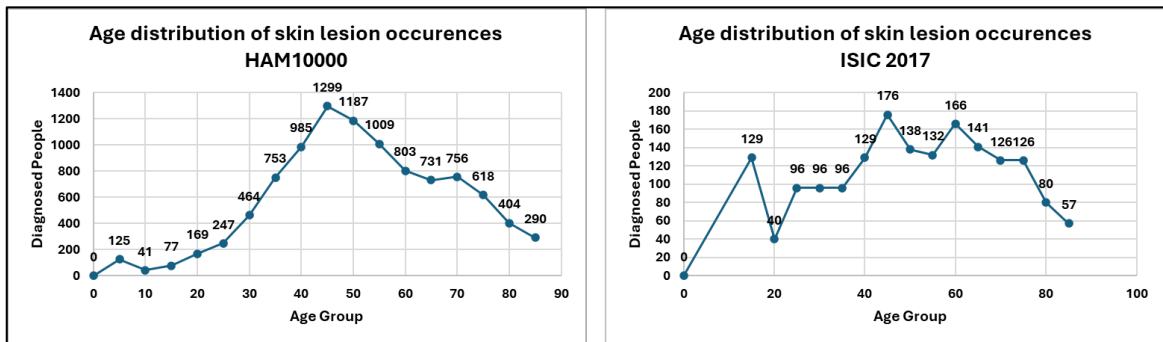


Figure 6. Age distribution of skin lesion occurrences

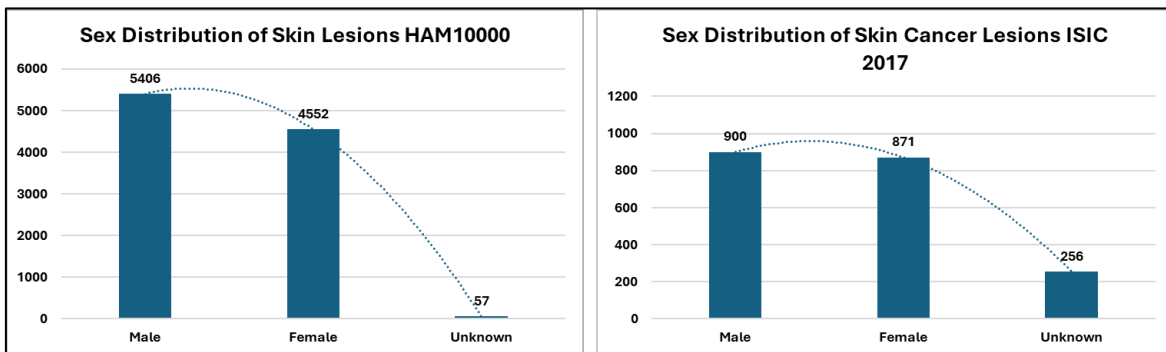


Figure 7. Sex distribution of skin lesion occurrences

### 2.3. Data and Model Generalization Techniques

The ability of an AI model to learn and accurately predict the pattern of previously unknown data or new information derived from the same distribution as the training data is generalized. Generalization refers to how successfully a model generalizes from training data to new data to analyze and make accurate predictions [45]. We used data and model generalization techniques to improve model performance and avoid overfitting and vanishing gradients, as shown in Figure 8. Modifying network structure by reducing the number of weights or network parameters, i.e., weight values, may suffice for deep networks. The data-centric technique focuses on data cleaning, data augmentation, feature normalization, and preparing appropriate validation and testing datasets—the model-centric methods, such as regularization and early stopping methods, are used to improve machine learning model performance during training and inference [46]. Figure 8 shows the pipeline flow for generalizing the data and model.

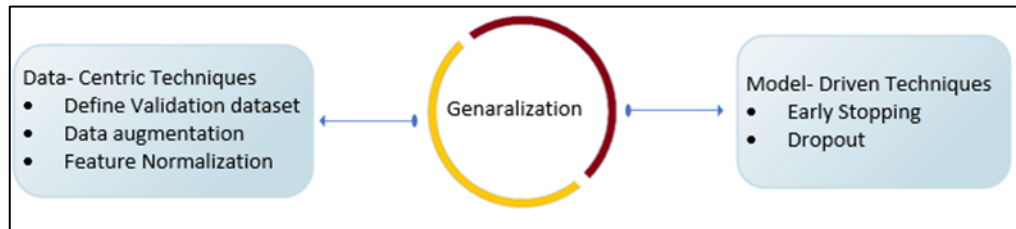


Figure 8. Generalization Technique Pipeline

#### 2.3.1 Validation Dataset

Predictive modelling begins with validating a dataset. A perfect validation set ensures a good depiction of real-world facts. As such, the machine learning model will be easy to test for generalization. The deep learning model should learn as many patterns as possible from a heterogeneous dataset. Data sample size affects model performance [47], [48]. Deep learning models in computer vision are trained on large datasets and images to improve model generalization. Hence, to enhance training dataset learning, cross-validation, whereby data is split into training, validation, and testing, would be beneficial. Cross-validation lets the model learn from the entire dataset while training and validating [49]. The data is divided into training and testing data for classification purposes, with 20% of the unique images used in testing. The remaining original data is divided into training and validation phases in an 80:20 ratio [25]. Table 3 depicts the data split for both datasets.

Table 3. Train and Test Dataset Split

Datasets	Training Data samples 80%	Validation Data samples 10%	Test Data samples 20%	Total Samples 100%
HAM 10000	6410	1602	2003	10015
ISIC 2017	1280	320	400	2000

#### 2.3.2 Data Augmentation

Data augmentation has become a crucial technique not only in natural image classification but also in melanoma classification. The main aim of data augmentation is to artificially increase the size of a training dataset by creating altered versions of the original data. It helps to reduce the issue of overfitting, which is often caused by having limited labelled data. This method is especially useful in medical image analysis, such as melanoma classification, where obtaining expert-annotated datasets can be challenging. Matsunaga et al. [50] applied data augmentation techniques to enhance the robustness of melanoma classification models by generating varied melanoma image versions, improving generalization to new data. González-Díaz [51] utilized rotation, scaling, and flipping for data augmentation to tackle overfitting in melanoma classification, creating a more diverse training set. Menegola et al. [52], [53] investigated the effect of data augmentation on deep-learning models for melanoma detection, demonstrating significant improvements in classification accuracy. Esteva et al. [10] highlighted the importance of data augmentation in training deep neural networks for skin cancer classification, using advanced techniques to capture the variability in skin lesion appearances. Codella et al. [36] focused on enhancing melanoma classification models through data augmentation, emphasizing the need to preserve the semantic integrity of augmented images to maintain label accuracy.

#### 2.3.3 Feature Normalization

The data is resized to 224 x 224 pixels at the end of Preprocessing. Each feature is normalized by subtracting the minimum data value from the mean of the data variable and then dividing it by the standard deviation. Thus, the pixels for each image are transformed to a range between 0 and 1 [19]. The z-score normalization technique normalizes the entire dataset by dividing it by 255, a grayscale image value [54].

$$Z - Score = \frac{(x-\mu)}{\sigma} \quad (1)$$

Where  $x$  is the original value,  $\mu$  is the mean of data, and  $\sigma$  is the standard deviation of data.

### 2.3.4 Early Stopping

Early stopping is a method for avoiding overfitting the model during training. A loss function is typically optimized by gradient descent as the model learns from the training dataset [55]. It occurs iteratively, as the model is trained over several epochs before it can converge. By terminating the model training when the validation loss exceeds a predetermined threshold, early stopping is utilized to avoid overfitting [56].

### 2.3.5 Dropout

Dropout [57] is a method of regularization in which the activation values of randomly chosen neurons are set to zero during training. This limitation forces the network to learn more stable features instead of depending on the ability of a small group of neurons to predict what will happen. The authors of [58] applied this study to convolutional networks with Spatial Dropout, which removes whole feature maps instead of just one neuron at a time.

### 2.3.6 One-hot Encoding

The one-hot encoding technique is used to represent the skin lesion categories of skin cancer by mapping the image to integer values where each class represents an integer value [25].

## 2.4 Feature Extraction

A crucial step in creating a machine-learning strategy for skin lesion analysis is feature extraction. Analyzing the features and patterns in the skin lesion image is a texture analysis. Techniques like the gray-level co-occurrence matrix are commonly used for feature extraction. Analyzing the color aspects of the skin lesion photographs is known as color analysis. The mean, standard deviation, skewness, entropy, gray Matrix, contrast, correlation, energy, and homogeneity are all components of the function we created. The description of the feature is expressed below [9]

**Mean:** The average intensity value of the pixels in a picture is revealed by the statistical measure known as the mean of the image. It is computed by adding the image's pixel values and dividing the total by the number of pixels. Mathematically, the following can be used to express an image's mean [9]:

$$mean = \left(\frac{1}{N}\right) \sum_{i=1}^N I(i) \quad (2)$$

For image analysis tasks like image classification, segmentation, and object recognition, the mean of a picture can be employed as a primary feature. For instance, when analyzing skin lesions, the mean intensity value of the lesion region might reveal details about the texture and pigmentation of the lesion, allowing for the differentiation of various skin lesion types.

**Standard Deviation:** The standard deviation is a statistical metric that sheds light on the distribution of intensity values of the image's pixels. It gauges how diverse or varied the image's pixel values are relative to their mean values. It is computed by first determining the average value of the picture and then computing the average of the squared disparities between the values of each pixel and the mean. The standard deviation number is then calculated by taking the square root of that average. The standard deviation of a picture may be expressed mathematically as [9]:

$$std = \sqrt{\left(\left(\frac{1}{N}\right) \sum_{i=1}^N (I(i) - mean)^2\right)} \quad (3)$$

**Skewness:** A statistical measure called skewness tells us if the distribution of intensity values among the pixels in the image is symmetric or asymmetric. It gauges how much the distribution is distorted from being normal. It is represented as:

$$skewness = \left(\frac{1}{N}\right) \sum_{i=1}^N \left(\frac{(I(i) - mean)}{std}\right)^3 \quad (4)$$

**Entropy:** Entropy is a statistical index that indicates the degree of ambiguity or unpredictability in a picture's distribution of pixel intensity values. It gauges how much information is included in an image. A more significant entropy number denotes more unpredictable and variable intensity levels, whereas a lower entropy value denotes predictable and consistent intensity values.

$$entropy = -\sum (p(i) * \log_2(p(i))) \quad (5)$$

Where  $p(i)$  is the likelihood that the image's intensity value  $i$  will occur.

Gray level co-occurrence matrix: A statistical matrix known as the gray level co-occurrence matrix (GLCM) offers details on the geographical distribution of intensity values of the image's pixel values. It counts how often two pixels with the same intensity value appear together and where they are with one another within a specific neighborhood [9].

Contrast: Contrast is a statistical measurement that sheds light on the variations in pixel intensity levels in a picture. It gauges how distinct the image's bright and dark regions are:

$$\text{contrast} = \frac{\max_{\text{intensity}} - \min_{\text{intensity}}}{\max_{\text{intensity}} + \min_{\text{intensity}}} \quad (6)$$

Correlation: A statistical measurement known as correlation sheds light on the linear correlation between the pixel intensity levels in a picture. It gauges how closely the pixel intensity levels are connected linearly. Correlation is given as:

$$\text{correlation} = \frac{\sum [(i - \mu_i)(j - \mu_j)p(i,j)]}{[\sigma_i \sigma_j]} \quad (7)$$

Energy: A statistical metric known as energy may be used to determine how uniform or homogeneous the distribution of intensity values among the pixels in a picture is. It quantifies the size of the squared components in the image's Gray Level Co-occurrence Matrix (GLCM). Which is represented as:

$$\text{energy} = \sum (p(i, j))^2 \quad (8)$$

Homogeneity: A statistical metric known as homogeneity may tell us how evenly or similarly the intensity values of the pixels in a picture are distributed. It assesses how closely related the intensity levels of the pixels are to one another [9].

$$\text{homogeneity} = \sum \left[ \frac{p(i, j)}{(1 + |i - j|)} \right] \quad (9)$$

## 2.5 Dense Convolutional neural network (DCNN)

Deep learning is an advanced approach for performing recognition tasks and extracting and abstracting visual information through multiple layers. Pattern recognition research has shown a growing interest in deep learning techniques, particularly convolutional neural networks (CNNs) [59]. A series of suggested networks have been proposed, including GoogLe-Net, ResNet, and DenseNet. DenseNet [60], with its innovative dense connection architecture, has notably outperformed many other deep learning models. DenseNet enables connections between any layers and uses skip connections to transfer information from shallow to deeper layers directly. This results in a more compact network with reduced feature redundancy. With all other parameters constant, convolutional network's convergence performance improves, and issues like degradation and gradient vanishing due to increased network depth are mitigated. Additionally, computational efficiency and the number of network parameters are significantly enhanced.

The initial step in DCNN is forward propagation, which includes assigning weights and applying activation functions to each neuron. Every neuron in each layer is connected with every other neuron in the next layer [61]. In a multi-layered feedforward network [62], forward and backward propagations are used to train the model, as shown in Figure 9.

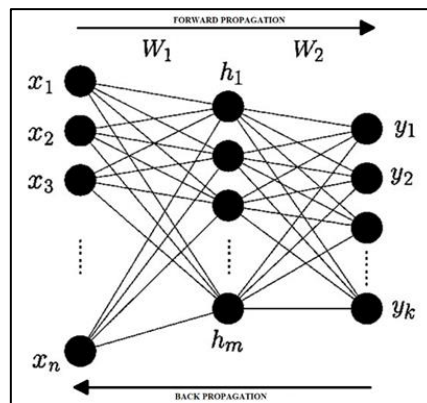


Figure 9. Dense Convolution Neural Network

The input data values are multiplied with their assigned weights, and bias will be added to overcome the zero output to the next neuron. Then, an activation function will be added at each neuron layer to prevent linearity. The output of the last neuron is the predicted value; forward propagation happens at each layer [37]. The neural network's output is compared to the desired output to check the loss during the training. The loss is calculated as [37]:

$$Loss = y - \hat{y} \quad (10)$$

$$y = w^T + bias \quad (11)$$

$$w^T = w_1x_1 + w_2x_2 + \dots + w_ix_i \quad (12)$$

where  $\hat{y}$  is the predicted value after the forward propagation.

The backpropagation algorithm is used to reduce the loss. In the backpropagation algorithm, the first step is to update the weights by applying the derivative chain rule. The weights are updated by backpropagating the decent gradient vector to reduce the loss [63]. Weights will be updated using equation 12, defined as:

$$w_{new} = w_{old} - \eta \frac{\partial Loss}{\partial w_{old}} \quad (13)$$

Where,  $w_{new}$  is the weight getting updated,  $w_{old}$  is the previous weight,  $\eta$  is the learning rate,  $\frac{\partial Loss}{\partial w_{old}}$  is to calculate the slope during gradient descent using the derivative chain rule.

During backpropagation and gradient-based learning, the vanishing gradient problem occurs when the slope values start to disappear [65]. To solve the vanishing descent problem in the middle layers, the ReLu activation function is used [62]. Also, in the last layer, the SoftMax activation function is used. Subsection 2.5.1 discusses how the proposed Dense Convolutional Neural Network is prominently used for image classification.

### 2.5.1 Improved Dense Convolutional Neural Network for Skin Lesion Classification

A Deep Convolutional Neural Network (DCNN) is widely utilized for image classification tasks. Illustrated in Figure 10, our proposed DCNN model is trained using a Dense Convolutional Neural Network via the Keras Sequential API to classify skin lesions. The architecture features a fully connected, multi-layered feedforward convolutional neural network designed to minimize the number of parameters while maintaining model quality. The model continuously learns higher-dimensional features, each receiving additional input from the preceding layer.

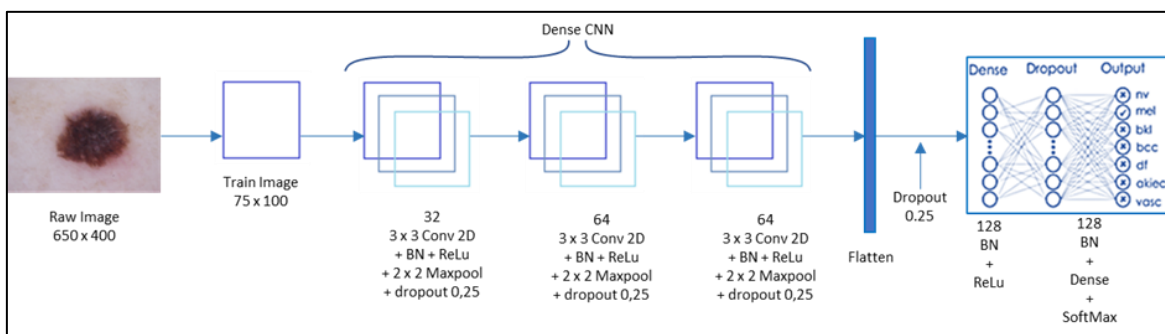


Figure 10. Proposed Dense Convolutional Neural Network

The raw images of resolution 650 x 400 were resized to 75 x 100 to be consistent with the model architecture to improve the image resolution, as shown in Figure 10. All the images have been normalized by 1./255 to improve the model's effectiveness. When we perform the convolution product using the vertical-edge filter, we can observe that the centre pixels in an image are used more and appear more often. Additionally, fewer pixels are visible on the image's corner edges than in the centre, which causes data loss at the edges and corners. We solved this issue by enclosing the image with padding, bringing the corner and edge pixels to the inner levels. In actual use, the image is padded with zeroes, and  $p$  represents the number of extra components added to either side of the image. We used stride to allow a step size for convolutional vector product. After

padding and stride, the images were fed into four convolutional 2D layers with repetitive 32, 64, and 64 filters. This method solves the vanishing gradient problem [65]. The kernel size of each CNN layer is 3 x 3. A mini-batch size 64 is utilized for normalization to decrease the number of training epochs and stabilize the neural network. Mathematically, we have for a given image and filter [18]:

$$\text{conv}(I, f)_{x,y} = \sum_{a=1}^{n_h} \sum_{b=1}^{n_w} \sum_{c=1}^{n_d} f_{(a,b,c)} I_{(x+a-1,y+b-1,c)} \quad (14)$$

Where  $n_h$  is the height,  $n_w$  is the width,  $n_d$  is the no of channels present in the image.

Also, the Rectified Linear Unit (ReLU) is used for the activation function of each neuron in the CNN layer [38] with a learning rate of 0.0001. ReLU activation function increases the sparsity of the neural network by converting the total values of the input to positive values as well as using less computational load [39]:

$$f(x)_{ReLU} = \max(0, x) \quad (15)$$

After the convolutional 2D layers, the resulting vector is flattened and passed to several fully connected layers with a dropout core block layer of value 0.25. The next layer is the dense layer, a fully connected neural network layer with 128 filters. The dropout layer follows with a parameter of 0.25. All the outputs in the classification must range between 0 and 1. Hence, the activation function for the final layer is SoftMax. The function SoftMax normalizes all the outputs in the final layer, summing it to 1. The mathematical equation of the SoftMax activation function is as follows [64]:

$$\sigma(\vec{z})_i = \frac{e^{z_i}}{\sum_{j=1}^K e^{z_j}} \quad (16)$$

Where  $z_i$  takes all real values of the input vector of the images and  $\sum_{j=1}^K e^{z_j}$  is the normalization function that sums up all the function's output values to 1, thus establishing a valid probability distribution.

The ADAM learning rate optimization algorithm proved to be the best optimizer to train the deep neural networks as it is speedy, converges rapidly, and resolves vanishing learning rates and high variance. ADAM stochastic optimization algorithm sets the decay to 0.9 and momentum to 0.999 [19]. Categorical cross-entropy is a loss function for single-label categorization in multiclass classification tasks.

## 2.6 Support Vector Machine (SVM)

A classifier for skin lesion analysis may be trained using the popular machine learning technique Support Vector Machine (SVM). A supervised learning technique called SVM can categorize pictures based on the characteristics that have been taken out of the images. It is crucial to remember that SVM is a computationally demanding algorithm that needs a lot of training data and the right feature extraction methods to work well [64]. It is also crucial to thoroughly preprocess the data to prevent overfitting and guarantee the model's generalizability [65]. SVM divides the data points into several classes by locating the best hyperplane. The choice of the hyperplane maximizes the distance between it and the nearest data points, sometimes referred to as support vectors[66].

## 2.7 K Nearest Neighbor (KNN)

KNN operates by locating a new data point's k-nearest neighbors in the feature space. Afterwards, the newly discovered data point is categorized into the class comprising most of its k-nearest neighbor [67]. To prevent ties, the value of  $k$  is often set to an odd number. KNN is a quick and efficient algorithm that can accurately classify skin lesions, mainly using suitable feature extraction methods and hyperparameter tweaking. KNN [68] can, however, require a lot of processing and may not scale effectively for massive datasets.

## 2.8 Decision Trees (DTs)

The decision tree is a well-liked machine learning approach for classification and regression issues. Recursively dividing the feature space into subsets according to the value of each feature is how the algorithm operates[69]. A tree-like structure is produced using this partitioning, with each node denoting a choice based on a feature and each branch denoting the decision's result. Decision trees [70] are a standard option for many machine-learning problems since they are easy to understand. Yet decision trees are susceptible to overfitting, which happens when the model gets too complicated and struggles with fresh data. Pruning and imposing restrictions on the model are two regularization strategies that can assist in minimizing overfitting and enhancing model performance.

### 3. RESULTS

The authors conducted simulation-based studies on various AI methods, including DCNN, SVM, KNN, and DT, rigorously evaluating them using publicly available datasets HAM10000 and ISIC2017. This section explains the simulation results of each AI model for skin cancer classification using performance metrics such as accuracy, sensitivity, specificity, and area under the ROC curve (AUC). The models follow a series of phases to classify skin lesions, including data acquisition, preprocessing, segmentation, feature extraction, and classification.

#### 3.1. Simulation Setup

This section set up a simulation environment to develop and simulate AI models. The hardware and software configuration included an Intel Core i7 processor operating at 4 GHz, an NVIDIA K80 GPU with 12 GB of GPU RAM and a performance capacity of 4.1 TFLOPS, and 64 GB of RAM, supplemented by SSD storage for efficient data retrieval and model storage. To effectively implement and train AI models, the latest version of Jupyter Notebook was utilized, running on the Windows operating system. Essential toolboxes such as the Deep Learning Toolbox, Statistics and Machine Learning Toolbox, and Parallel Computing Toolbox were employed. Additionally, the appropriate version of the NVIDIA CUDA toolkit, compatible with GPU, was installed alongside the latest GPU drivers.

#### 3.2. Dataset Description

The simulation environment setup begins with meticulous data preparation, involving the selection of datasets encompassing a diverse range of dermoscopy images of skin lesions. Acquiring raw data from various image modalities is crucial, whether manually collected from hospitals and patients or sourced from publicly available web datasets. The quality of input data significantly impacts the speed and accuracy of the disease detection process. Most dermoscopic datasets are freely available on open databases.

Cassidy et al. [37] analyzed dermoscopy datasets and found that ISIC datasets are primarily used for binary classification and segmentation tasks. They noted that classification accuracy might suffer in smaller datasets, which are often skewed and contain repeated images, increasing overall dataset size. Eliminating duplicate images before inputting them into a neural network can enhance classification accuracy and reduce computation time and cost. Large datasets have been shown to improve AI model performance. However, the limited quantity and variety of dermatoscopic image datasets pose challenges in training neural networks for automated diagnosis of pigmented skin lesions [34].

To address this, the authors gathered dermatoscopic images from diverse populations and various modalities from two publicly available datasets, HAM10000 [38] and ISIC2017 [39], for this study. Due to this heterogeneity, data-centric generalization techniques were employed, including data augmentation, oversampling of under-represented groups, and feature normalization. Furthermore, semi-automatic procedures utilizing specially trained neural networks were implemented.

#### 3.3 Performance System of Measurement

This study used the following standard precision metrics for the evaluation of the training model, developed from True Positive (TP), True negative (TN), False positive (FP), and False negative (FN) predictions [9]:

1. Accuracy reflects the number of correct predictions (TP and TN) and overall predictions (TP + FP + TN + FN).

$$accuracy = \frac{TP+TN}{TP+FP+TN+FN} \quad (17)$$

2. Precision indicates true positive probability in all positive prediction cases. If the prediction is 1, all positive predictions are truly positive; however, positive samples are still incorrectly predicted as negative.

$$precision = \frac{TP}{TP+FP} \quad (18)$$

3. Recall the contrast precision as it indicates the probability of truly being negative when the prediction is negative. Similarly, if the recall is 1, all negative predictions are truly negative; however, negative samples are still incorrectly predicted as positive.

$$recall = \frac{TP}{TP+FN} \quad (19)$$

4. F1-Score establishes a balance between Precision and Recall. More advanced than accuracy, the F1-score focuses on true positive values and is a better measurement for imbalance distribution classes.

$$f1 - score = \frac{2TP}{2TP+FP+FN} \quad (20)$$

5. Specificity indicates how well the model can detect negatives and the proportion of true negatives the model correctly predicts. In this problem, sensitivities are usually high due to the highly imbalanced dataset.

$$specificity = \frac{TN}{FP+TN} \quad (21)$$

### 3.4 Simulated Outcomes

The primary objective of this study was to develop a robust model for classifying skin cancer. The process starts by acquiring raw data and selecting datasets that consist of diverse dermoscopy images of skin lesions, as discussed in section 3.2.

After acquiring the raw data, the datasets were split into training and testing subsets in an 80:20 ratio to ensure a balanced and unbiased evaluation. Following the data splitting, preprocessing steps were applied, such as normalizing pixel values to a standard scale to maintain consistency across the dataset. Additionally, data augmentation techniques rotation, flipping, and zooming were used to increase data diversity and enhance the robustness of the AI models.

Next, Otsu's method was employed for image segmentation, a critical step for isolating regions of interest within the dermoscopy images, facilitating more accurate feature extraction. Features were then extracted using the Gray Level Co-occurrence Matrix (GLCM) method, which captures essential texture information for classification.

The extracted features were used to train various AI models, including Deep Convolutional Neural Networks (DCNNs), K-nearest neighbor (KNN), Support Vector Machines (SVMs), and Decision Trees (DTs). During the training phase, early stopping and model checkpoints were utilized to prevent overfitting and ensure that the models generalized well to unseen data.

Once the models were trained, their performance was evaluated on the validation subset using key metrics, as discussed in section 3.3. We selected the model demonstrating the best performance across these metrics for further validation.

In the final validation step, the selected model was assessed using the testing subset to evaluate its generalization capabilities and overall accuracy. This step is crucial to ensure the model performed well on new, unseen data, confirming its reliability for practical applications in skin lesion classification.

#### 3.4.1 Data Augmentation

Data augmentation is a crucial strategy employed to enhance the accuracy and efficiency of machine learning models. By generating variations of the original dataset, data augmentation effectively increases the dataset's apparent size, allowing for the development of advanced models using limited training data without compromising accuracy. This technique also helps balance the dataset through oversampling, where the sample size of the smallest class is increased to match that of the largest class. After achieving a balanced dataset, various augmentation methods are applied to the training set images, including horizontal and vertical flipping, rotation, random cropping, adjustments to contrast and brightness, random shearing, rescaling, and shifting in width and height. These augmentation techniques enrich the dataset and mitigate the risk of overfitting by exposing the model to a broader range of scenarios. Table 4 details the specific data augmentation parameters utilized to address the constraints posed by the limited number of labelled images available in the datasets, and the augmented images are shown in Figure 11.

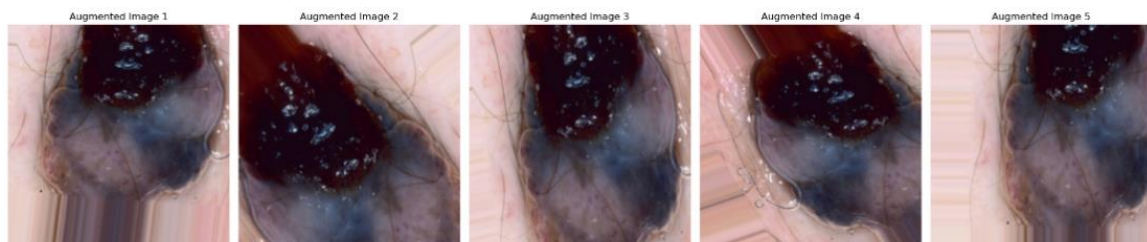


Figure 11. Data augmentation

Table 4. Data Augmentation Parameter

Parameters	Values	Action
Rescale	1./255	Modifying the dimensions of the image
Rotation Range	90	Allows random rotation of data generated between the ranges 10 to -10.
Width Shift Range	0.1	Shifts the image horizontally by 0.1.
Height Shift Range	0.1	Shifts the image vertically by 0.1.
Shear Range	10	The image is stretched slantly by a factor of 0.1.
Horizontal Flip	True	The image is flipped randomly across a horizontal direction
Vertical Flip	True	The image is flipped randomly across the vertical direction.
Fill Mode	Nearest	Chooses the nearest pixel to fill the empty values.

### 3.4.2 Image Preprocessing and Segmentation

Figure 12 sequentially demonstrates the preprocessing steps applied to a skin lesion image to prepare it for feature extraction and analysis. The process begins with the original image, depicting the raw skin lesion with natural artefacts. This image is then resized to a fixed dimension of 224 x 224 pixels to ensure uniformity. Next, the resized image is normalized by scaling pixel values to the [0, 1] range, improving the performance of learning algorithms. Following normalization, a median filter is applied to reduce noise while preserving edges, resulting in a smoother image. The median-filtered image is converted to grayscale, simplifying it to a single channel, which is essential for many image processing techniques. Subsequently, a bottom hat filter highlights dark regions against a light background, enhancing the contrast of features like hair and other artefacts. It is followed by binarization to create a binary mask, separating the foreground from the background, and dilation to fill small gaps and connect features. The hair removal step is applied with the surrounding skin color, producing a cleaner image. Finally, Otsu's thresholding is applied to the hair-removed image to determine the optimal threshold to separate the lesion from the background, enhancing the region of interest for further analysis. Each step progressively refines the image, making it more suitable for accurate feature extraction and subsequent analysis, which is crucial in skin lesion classification and diagnosis.

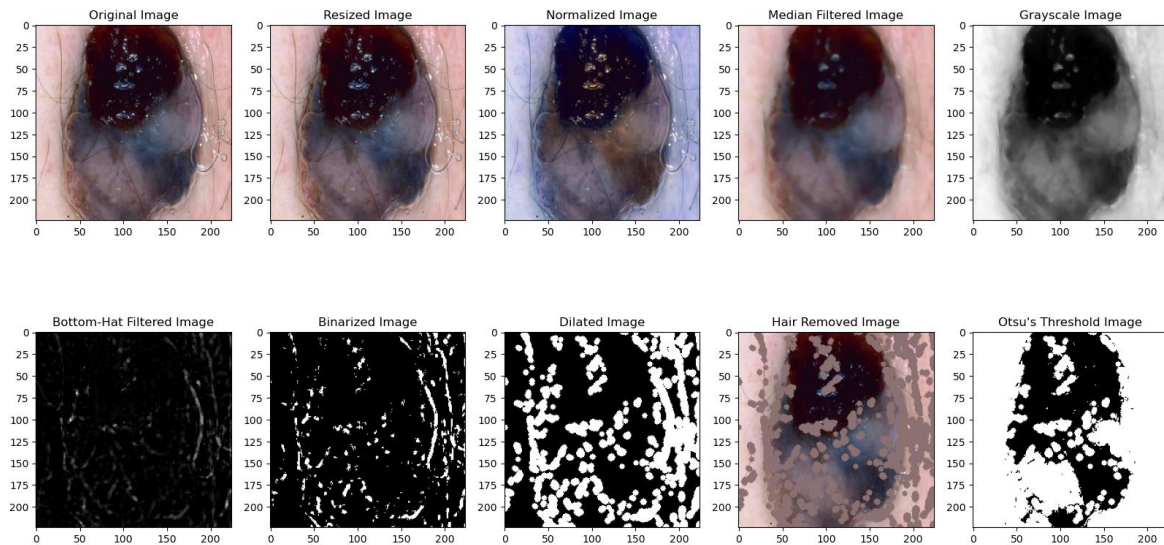


Figure 12. Images after performing preprocessing and segmentation

### 3.4.3 Feature Extraction

In Figure 13, the GLCM features extracted from the image provide a detailed understanding of its texture characteristics. The contrast value of 2.7 indicates significant local variations and a detailed texture, suggesting noticeable differences in intensity between neighbouring pixels. The dissimilarity value 1.3 suggests a complex texture characterized by substantial variations among pixel pairs, indicating a high degree of texture complexity. With a homogeneity value of 0.7, the texture appears uniform with some variation rather than highly uniform. The energy value of 0.5 indicates moderate texture uniformity, suggesting that the pixel values exhibit a degree of consistency but are not perfectly uniform. A correlation value 0.6 suggests a moderate positive correlation between pixel pairs, indicating some regular patterns but not a solid linear dependency. Lastly, the ASM value of 0.4 reflects a moderate level of texture uniformity, indicating some consistency but also variability in the texture. Figure 13 presents the spatial relationship of pixels.

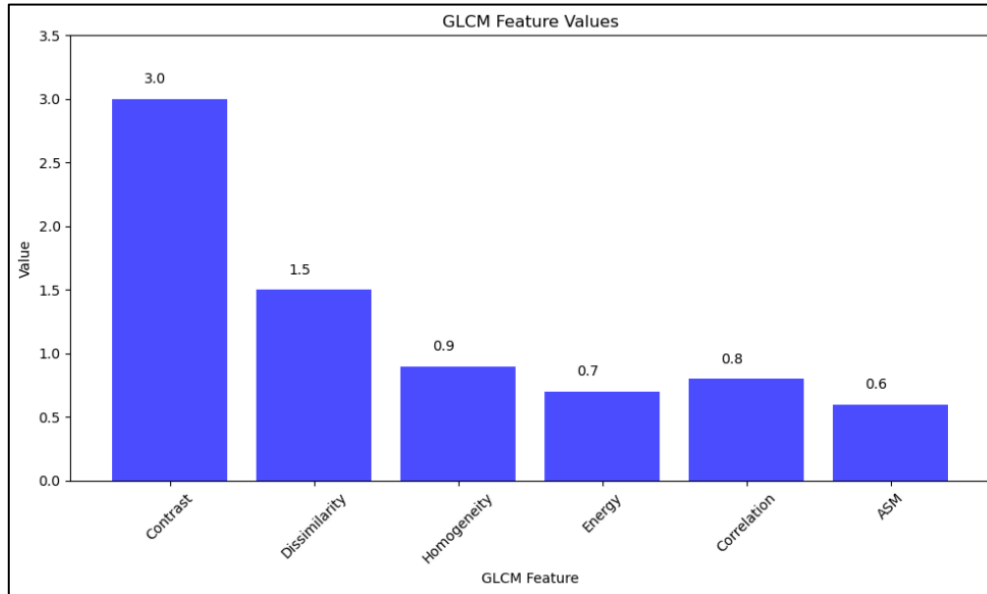


Figure 13: GLCM Feature values

### 3.4.4 Classification

The images obtained from the feature extraction phase are subsequently fed into classifiers to predict the nature of skin lesions. In our study, we utilized Deep Convolutional Neural Networks (DCNN), K-Nearest Neighbors (KNN), Support Vector Machines (SVM), and Decision Trees (DT) for this classification task. Each Classifier brings unique strengths to the analysis, enabling a comprehensive evaluation of their effectiveness in accurately identifying skin lesions. A range of performance metrics are employed to evaluate these models' ability to apply to new or unfamiliar data, as discussed in section 3.3.

#### 3.4.4.1 DCNN Results

The DCNN model is trained on the HAM10000 and ISIC 2017 datasets for 50 epochs after data augmentation and normalization. It is essential to mention that the choice for the number of epochs used in our study is a trade-off between computational cost and prediction or classification accuracy. However, after several independent batches of training, it is justified that the 50 epochs provide a tenable classification accuracy. The classification accuracy of the proposed DCNN model during the training phase with 80% of the dataset is 97.01% for HAM10000 and 96.89% for ISIC 2017, as shown by the blue plot in Figures 5 and 6. The learning curve of the proposed DCNN is shown by the validation accuracy (orange plot) in Figures 14(a) and 15(a), which is inversely proportional to the validation loss shown in Figures 14(b) and 15(b) on HAM10000 and ISIC 2017 datasets. These results indicate that the DCNN satisfactorily learns the unique features the datasets represent for accurate classification and generalization to other datasets.

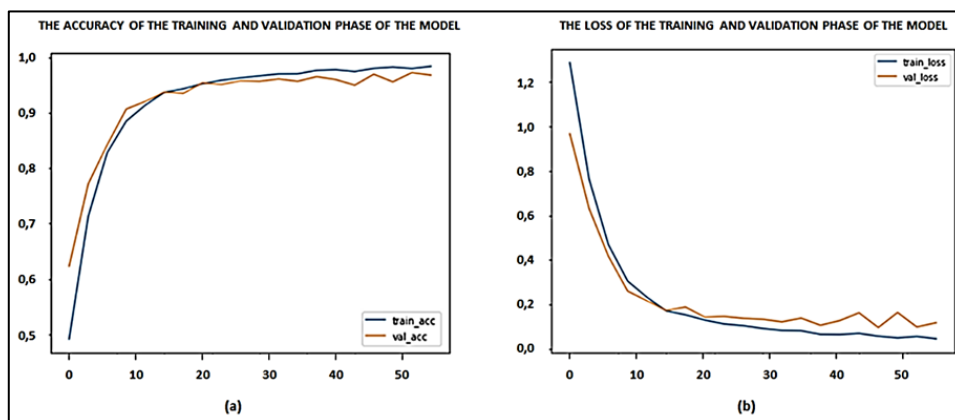


Figure 14. (a) Accuracy (b) Loss of the Training and Validation data of the Model - HAM10000 dataset

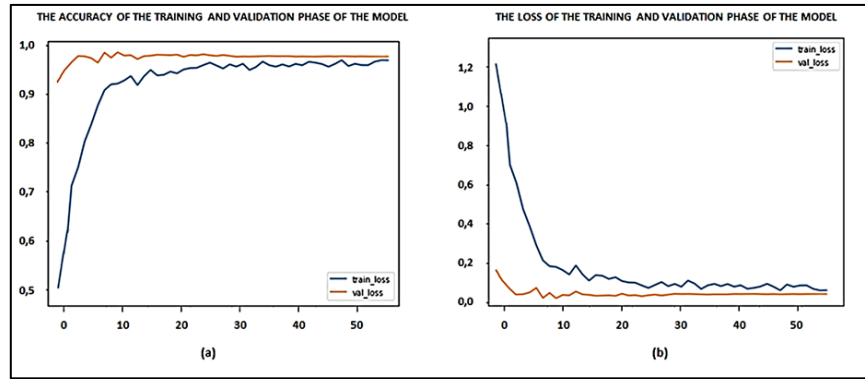


Figure 15. (a) Accuracy (b) Loss of the Training and Validation data of the Model -ISIC 2017 dataset

The confusion matrix of the DCNN-based skin lesion classification model for HAM10000 and ISIC 2017 datasets for the training phase is shown in Figures 16(a) and 17(a), and the testing phase is depicted in Figures 16(b) and 17(b). It can be observed from the diagonal elements of the matrices (true positive classification) that the proposed DCNN model correctly classifies the different kinds of skin lesions with a very high degree of accuracy and negligible misclassification.

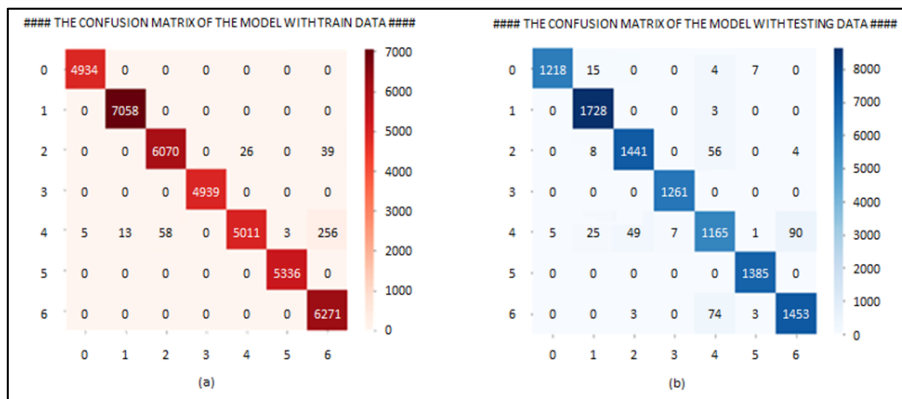


Figure 16. HAM10000 Dataset - Confusion Matrix (a) with Training Data (b) with Testing Data



Figure 17. ISIC 2017 - Confusion Matrix (a) with Training Data (b) with Testing Data

Using the metrics presented in Section 3.3, Table 5 and Figure 18 illustrate the performance analysis of the proposed DCNN for correctly classifying the various types of skin lesions from HAM10000 and ISIC 2017 datasets. The model's precision to correctly classify the skin lesion is between 94%-100 for DF, BKL, MEL, NV, VASC, BCC, and BN. At the same time, the ACKIEC and SK produce a precision of 89%. Generally, the proposed DCNN model marginally classifies the ACKEIC skin lesion with an F1 score of 88% compared to the VASC and BCC, with a maximum F1 score. The suggested DCNN model's overall classification accuracy for HAM10000 and ISIC 2017 is 97.01% and 96.89%, respectively. As a result, the DCNN model would generalize effectively and perform well for practical application when used to classify datasets of skin lesions.

Table 5. Performance Analysis of the DCNN Model

Dataset	Skin Lesions	Precision (%)	Recall (%)	F1-Score (%)	Avg. accuracy (%)
HAM10000 Dataset	ACKIEC	89	87	88	97.01
	DF	94	95	94	
	BKL	97	95	96	
	MEL	97	100	99	
	NV	100	98	99	
	VASC	99	100	100	
	BCC	99	100	100	
ISIC 2017 Dataset	MEL	97	100	99	96.89
	SK	89	87	88	
	BN	100	98	99	

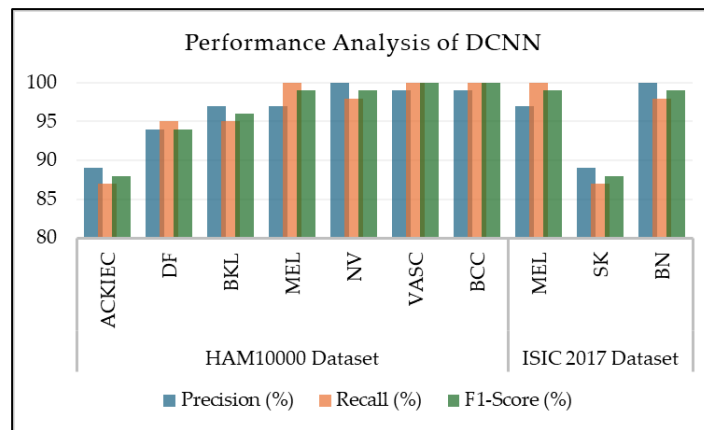


Figure 18. Performance Analysis of the DCNN Model

### 3.4.4.2 SVM Outcomes

Table 6 and Figure 19 show that the SVM model has an accuracy of 87.75% for identifying benign and malignant classes. Precision, F1-score, and recall values for the two classes examined range from roughly 83% to 96%.

Table 6. SVM Performance Outcomes

Dataset	Skin Lesions	Precision (%)	Recall (%)	F1-Score (%)	Avg. accuracy (%)
HAM10000 Dataset	ACKIEC	83	85	84	87.75
	DF	78	80	79	
	BKL	88.5	89.23	87.5	
	MEL	92	94	93	
	NV	95	96	95.5	
	VASC	79	75	77	
	BCC	85	87	86	
ISIC 2017 Dataset	MEL	81.80	79.80	80,66	85.00
	SK	79	80	78.6	
	BN	78	80	79	

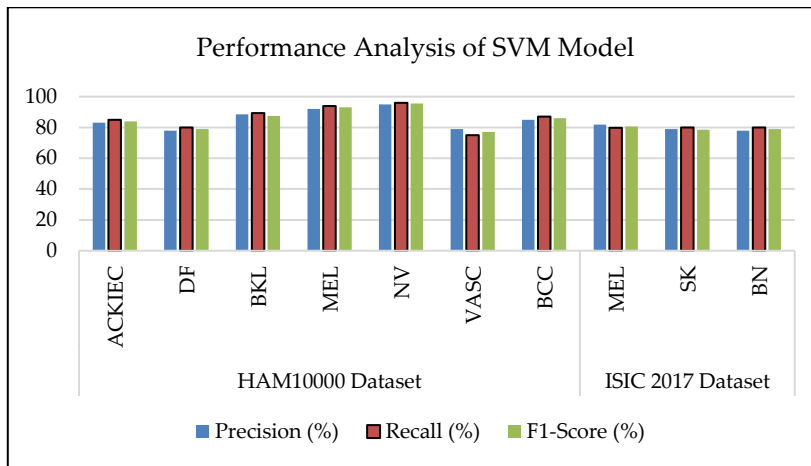


Figure 19. Performance Analysis of the SVM Model

3.4.4.3 KNN Outcomes

From Table 7, the KNN model classifies skin lesions with an accuracy of 93.03% for HAM10000 and 92.8 for ISIC2017 datasets. Figure 20 shows the performance analysis of KNN.

Table 7. KNN Performance Outcomes

Dataset	Skin Lesions	Precision (%)	Recall (%)	F1-Score (%)	Avg. accuracy (%)
HAM10000 Dataset	ACKIEC	85.2	88.3	86.7	93.03
	DF	78.0	82.5	80.2	
	BKL	90.1	92.4	91.2	
	MEL	93.3	94.6	94	
	NV	95.5	96.2	95.8	
	VASC	84.7	83	83.8	
	BCC	88.4	89.9	89.1	
ISIC 2017 Dataset	MEL	91.0	90.5	90.8	92.8
	SK	79.5	77.8	78.6	
	BN	82.1	80.9	81.5	

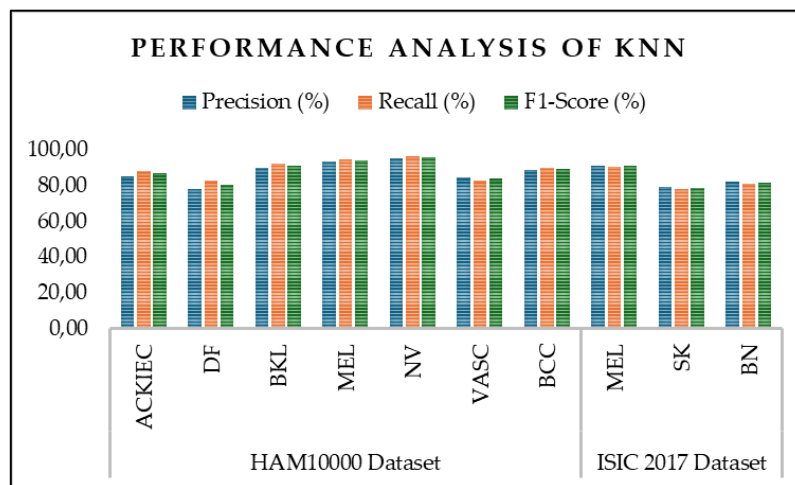


Figure 20. Performance Analysis of the KNN Model

#### 3.4.4.4 Decision Tree Outcomes

The decision tree model classifies skin lesions from Table 8 with an accuracy of 90.58%. The results show that precision and F1-scores are high for malignant, with 96.45 % and 91.10 %; recall obtained a high score for benign, with 95.87%. Figure 21 shows the performance of DTs.

Table 8. Decision Tree Performance Outcomes

Dataset	Skin Lesions	Precision (%)	Recall (%)	F1-Score (%)	Avg. accuracy (%)
HAM10000 Dataset	ACKIEC	84	86.5	85.2	90.58
	DF	78.5	81	79.7	
	BKL	89.3	90.1	89.7	
	MEL	96.5	95.8	91.10	
	NV	96.2	94.7	95.4	
	VASC	85.7	84.3	85	
	BCC	90	88.6	89.3	
ISIC 2017 Dataset	MEL	91.8	90	90.9	89.52
	SK	80.4	82.6	81.5	
	BN	87.58	85.9	86.7	

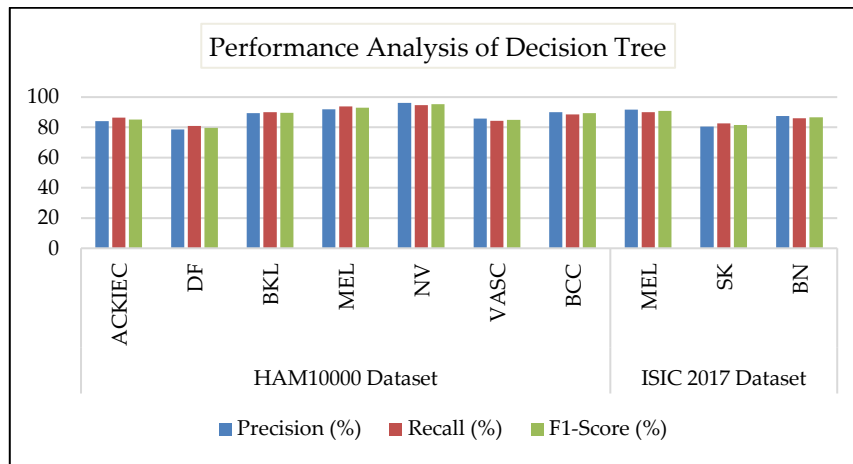


Figure 21. Performance Analysis of the Decision Tree Model

## 4. DISCUSSION

### 4.1 Comparative Analysis of AI-Based Models

The results show that the DCNN method accurately classifies skin lesions. Although data augmentation methods like rotation, scaling, and flipping can expand dataset size, the improved strategy goes above and beyond standard methods. It extracts high-quality images where data is missing or unbalanced datasets, improving the model's ability to generalize to different lesion types. The DCNN Classifier outperforms classic machine learning classifiers such as SVM, KNN and Decision trees in various ways. It combines the ability of DCNN to automatically learn discriminative features from raw image data with the potential of deep learning to achieve improved generalization, robustness, and accuracy rates. Skin lesions' enormous diversity and complexity may challenge handmade feature extraction methods such as texture analysis or colour-based descriptors, which rely on domain-specific knowledge. The DCNN automatically learns and extracts critical features from skin lesion images, eliminating the need for manual feature engineering. The DCNN can handle differences in lesion appearance, illumination, and image quality due to its improved generalization abilities. As a result, classification performance is more robust and consistent even on novel or tough datasets. It can enhance training datasets and allow researchers to analyze sparse or unavailable lesion samples. It has a high accuracy of 97.10% and 97.16% for precision, recall, and F1-Score, demonstrating that it can detect and differentiate between different skin lesions. The Classifier is particularly

flexible to visual contrasts between lesions for precise diagnosis and classification. It solves problems such as class imbalance, annotated data, overfitting, and generalization to new models by capitalizing on DCNN. Figure 22 shows the comparative analysis of AI-based models.

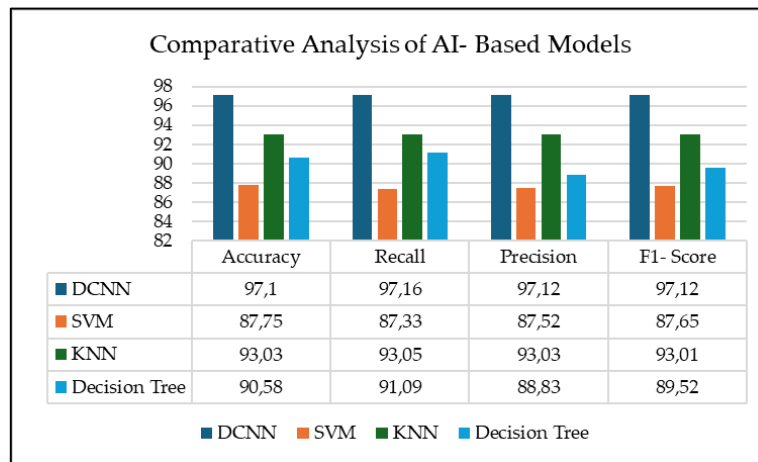


Figure 22. Comparative Analysis of AI-Based Models

Despite achieving high accuracy, this study had limited capacity to fine-tune its hyper-parameters. Consequently, conducting all the necessary tests to fine-tune our model took considerable time. The most problematic aspect of this study was the duration of each training session, mainly when training was more than 50 epochs. It significantly complicated the difficulty of fine-tuning the DCNN on the dataset.

#### 4.2 Comparison with the State-of-the-art Methods

In this section, we have also compared the DCNN model to various state-of-the-art approaches to validate its robustness and accuracy, as demonstrated in Table 6. The DCNN model outperformed state-of-the-art methods, improving skin lesion classification accuracy. The aim of employing the DCNN model was to solve the vanishing gradient problem and train faster with fewer parameters. Research shows that the accuracy varies with different datasets due to variations in color, illumination, sizes, and resolution of the images [35]. Using the HAM10000 dataset for multiclass skin lesion classification, Afza et al. [1] obtained 94.36% using HWO & EMI model architecture, Hemsı et al. [16] achieved 84% using CNN with space shifting technique, Ameri [19] achieved 84% using AlexNet, Kondaveeti, et al. Modified ResNet50 achieved 90% [71]. The model Quantization Technique gave Maiti et al. [72] 86.5% accuracy. ISIC and PH2, binary classifications by [1], [2], [30], [31], [73], had lower accuracy rates than the suggested DCNN model, shown in Table 9. Figures 23 and 24 show the comparison of DCNN with state-of-the-art methods for two datasets.

Table 9. Comparison of the proposed model accuracy with state-of-the-art methods

Author	Classification Models	Dataset	Accuracy (%)
[1]	HWO-ELM based classification	HAM 10000	93.40
[16]	CNN with Space Shifting Technique	HAM 10000	84
[18]	CNN	HAM 10000	83.11
[19]	AlexNet	HAM 10000	84
[22]	Lesion Classifier	ISIC 2017	95
[25]	RCNN	ISIC 2017	95.2
[26]	F-RCNN and SVM	ISIC 2017	89.1
[27]	CSLNet	ISIC 2017	90
[29]	Mask-RCNN and DenseNet	ISBI2017	94.80
		HAM10000	88.50
[30]	LCNet DCNN Classifier	ISIC 2017	88.23
[36]	Modified ResNet50	HAM 10000	90
[38]	Conventional CNN	ISIC Archive	84.76
[37]	Model Quantization Technique	HAM 10000	86.5
[74]	Deep CNN	HAM 10000	85.80
[75]	ResNeXt101	HAM 10000	92.83
	DCNN Model	HAM 10000	97.01
		ISIC 2017	96.89

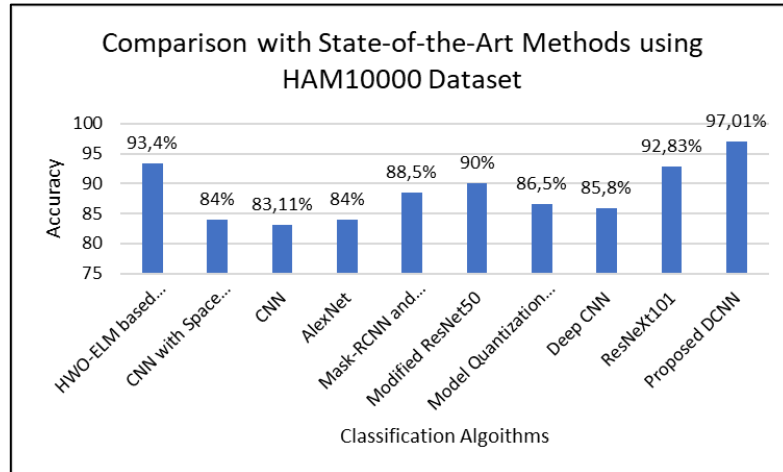


Figure 23. Comparative analysis of DCNN based on the accuracy for HAM 10000 Dataset

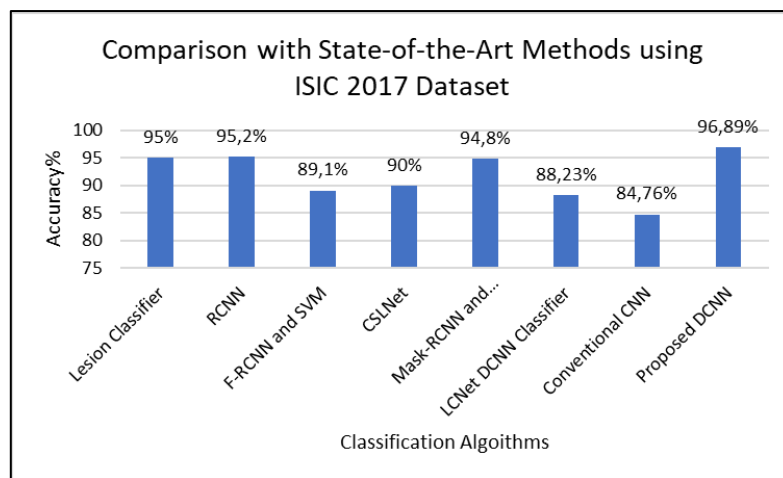


Figure 24. Comparative analysis of Dense CNN based on the accuracy for ISIC 2017 Dataset.

## 5. CONCLUSION AND FUTURE RESEARCH

Skin cancer is hazardous and has a low survival probability if detected earlier. Experts are under much strain because of the prevalence of diagnostic errors in manual examinations. There has been a rise in the pursuit of automated Skin cancer detection technologies, which can help doctors make more informed diagnoses. Therefore, this study provides a potentially significantly improved approach for detecting and classifying skin cancer at an early stage. To accomplish robust learning and feature representation of the various classes of skin lesions, the DCNN model comprises a series of convolutional neural networks stacked together. We used the HAM10000 and ISIC 2017 datasets, which contain multi-source dermoscopic images of common pigmented lesions, to detect and classify skin lesions. The class imbalance was resolved using data augmentation and normalization techniques. We compared our model's accuracy, precision, recall, and F1 score to state-of-the-art approaches to demonstrate our model's efficacy. Using HAM10000, our suggested model performed better than the previous models, with a 97% classification accuracy, 96.43% precision, 96.57% recall, and an F1-Score of 96.57%. For ISIC 2017 F1-Score, Precision and recall achieved 95%. The results show that the proposed method can be used for practical applications for medical diagnosis in real-time skin cancer detection and identification. The current results have provided a basis for using additional data sets so that further insight can be drawn and any possible generalization of these results over several data sets can be possible. In addition, the suggested model has only been trained and evaluated for 50 epochs due to hardware constraints, which artificially lowers the model's accuracy but leaves room for improvement in future studies. Future work will involve verifying the approach on more extensive datasets, improving the model to make it more generalized and amenable to cross-platform deployment, and testing the model on other datasets

**ACKNOWLEDGMENTS**

This research received no external funding.

**Appendix A**

Author	Year	Classification Algorithm	Dataset	Classification Type	Accuracy (%)	Precision (%)	Recall (%)	F1-Score (%)	Limitations
[1]	2022	HWO-ELM based Classification	HAM10000 ISIC 2018	Multiclass	93.40 94.36				Performance need improvement
[2]	2022	Ensemble ML and VGG16, ResNet	ISIC 2018	Binary	92	91	92	83	This method is computationally complex
[6]	2022	CNN and SVM	ISIC CPTAC- CM	Binary	99.8 99.9				Despite high accuracy, this model fails to classify the images correctly and makes erroneous Classifications.
[20]	2021	CNN with Space Shifting Technique	HAM 10000	Multiclass	84	76.6	65.6	95.4	This method is computationally complex.
[21]	2021	CNN	ISIC 2018	Multiclass	79.45	76	78	76	Performance need improvement
[22]	2021	CNN	HAM 10000	Multiclass	83.11	81.86	80.50	82.80	Performance need improvement
[23]	2020	AlexNet	HAM10000	Binary	84	81	88		Time-consuming, used a small dataset
[26]	2019	Lesion Classifier	PH2 ISIC 2017	Binary	95		97		
[31]	2021	RCNN	ISIC 2016, ISIC 2017, PH <sup>2</sup>	Binary	95.40 95.2 96.1		90.0 86.1 97.0		This method is computationally complex.
[32]	2021	F-RCNN and SVM	ISIC 2016 ISIC 2017	Binary	89.1		85.9		Performance need improvement
[33]	2020	CSLNet	ISIC 2017 ISIC 2018 ISIC 2019	Multiclass	90	91	90		Validation improvement is required with more clinical information on subjects.
[35]	2021	Mask-RCNN and DenseNet	ISBI 2016 ISBI2017 HAM10000	Multiclass	96.30 94.80 88.50	96.44 95.00 88.66	96.25 94.80 88.54	96.34 94.90 88.60	
[37]	2022	LCNet DCNN Classifier	ISIC 2016 ISIC 2017 ISIC 2020 PH <sup>2</sup>	Binary	81.41 88.23 90.42 76.00	81.8 78.5 90.4 67.8	81.3 87.8 90.3 75.3		This model has an advantage over small datasets but requires improvement for large datasets, and it is computationally complex.
[38]	2021	SqueezeNet DCNN	PH <sup>2</sup>	Binary	92.18	80.77	95.1	80.84	Performance need improvement
[61]	2020	Conventional CNN	ISIC Archive	Binary	84.76	91.97	78.71		Performance need improvement

[65]	2020	Modified ResNet50	HAM 10000	Multiclass	90	89	90		Performance need improvement
[68]	2021	Model Quantization Technique	HAM 10000	Multiclass	86.5	93.0	93.0	93.0	The model's accuracy decreased by 6.5% compared to the base model.

## REFERENCES

- [1] F. Afza, M. Sharif, M. Attique Khan, U. Tariq, H.-S. Yong, and J. Cha, "Multiclass Skin Lesion Classification Using Hybrid Deep Features Selection and Extreme Learning Machine," 2022, doi: 10.3390/s22030799.
- [2] I. A. Alfi, M. M. Rahman, M. Shorfuzzaman, and A. Nazir, "A Non-Invasive Interpretable Diagnosis of Melanoma Skin Cancer Using Deep Learning and Ensemble Stacking of Machine Learning Models," *Diagnostics*, vol. 12, no. 3, pp. 1–18, 2022, doi: 10.3390/diagnostics12030726.
- [3] J. De Wet, M. Steyn, H. F. Jordaan, R. Smith, S. Claasens, and W. I. Visser, "An Analysis of Biopsies for Suspected Skin Cancer at a Tertiary Care Dermatology Clinic in the Western Cape Province of South Africa," *J. Skin Cancer*, vol. 2020, 2020, doi: 10.1155/2020/9061532.
- [4] C. Jen Ngeh, C. Ma, T. Kuan-Wei Ho, Y. Wang, and J. Raiti, "Deep Learning on Edge Device for Early Prescreening of Skin Cancers in Rural Communities," *2020 IEEE Glob. Humanit. Technol. Conf. GHTC 2020*, 2020, doi: 10.1109/GHTC46280.2020.9342911.
- [5] C. Y. Wright, D. Jean du Preez, D. A. Millar, and M. Norval, "The epidemiology of skin cancer and public health strategies for its prevention in southern Africa," *Int. J. Environ. Res. Public Health*, vol. 17, no. 3, 2020, doi: 10.3390/ijerph17031017.
- [6] A. G. Diab, N. Fayeze, and M. M. El-Seddek, "Accurate skin cancer diagnosis based on convolutional neural networks," *Indones. J. Electr. Eng. Comput. Sci.*, vol. 25, no. 3, pp. 1429–1441, 2022, doi: 10.11591/ijeecs.v25.i3.pp1429-1441.
- [7] FTI Consulting, "Overview of the health technology sector in South Africa: Opportunities for collaboration," 2019. [Online]. Available: <https://www.rvo.nl/sites/default/files/2021/03/Overview-of-the-health-technology-sector-in-South-Africa-Opportunities-for-collaboration.pdf>.
- [8] J. M. Kabongo, S. Nel, and R. D. Pitcher, "Analysis of licensed South African diagnostic imaging equipment," *Pan Afr. Med. J.*, vol. 22, pp. 1–9, 2015, doi: 10.11604/pamj.2015.22.57.7016.
- [9] K. Behara, E. Bhero, J. T. Agee, and V. Gonela, "Artificial Intelligence in Medical Diagnostics: A Review from a South African Context," *Sci. African*, p. e01360, 2022, doi: 10.1016/j.sciaf.2022.e01360.
- [10] A. Owoyemi, J. Owoyemi, A. Osiyemi, and A. Boyd, "Artificial Intelligence for Healthcare in Africa," *Front. Digit. Heal.*, vol. 2, no. July, 2020, doi: 10.3389/fgdh.2020.00006.
- [11] K. York *et al.*, "Primary cutaneous malignancies in the Northern Cape Province of South Africa: A retrospective histopathological review," *South African Med. J.*, vol. 107, no. 1, pp. 83–88, 2017, doi: 10.7196/SAMJ.2017.v107i1.10924.
- [12] A. N. Hoshyar, A. Al-Jumaily, and A. N. Hoshyar, "The beneficial techniques in preprocessing step of skin cancer detection system comparing," *Procedia Comput. Sci.*, vol. 42, no. C, pp. 25–31, 2014, doi: 10.1016/j.procs.2014.11.029.
- [13] M. S. Madarkar and V. R. Koti, "Fotofinder dermoscopy analysis and histopathological correlation in primary localized cutaneous amyloidosis," *Dermatology Pract. Concept.*, vol. 11, no. 3, pp. 1–7, 2021, doi: 10.5826/dpc.1103a57.
- [14] V. Narayanamurthy *et al.*, "Skin cancer detection using non-invasive techniques," *RSC Adv.*, vol. 8, no. 49, pp. 28095–28130, 2018, doi: 10.1039/c8ra04164d.
- [15] D. A. Okuboyejo and O. O. Olugbara, "A Review of Prevalent Methods for Automatic Skin Lesion Diagnosis," *Open Dermatol. J.*, vol. 12, no. 1, pp. 14–53, 2018, doi: 10.2174/187437220181201014.
- [16] K. Thurnhofer-Hemsi, E. Lopez-Rubio, E. Dominguez, and D. A. Elizondo, "Skin lesion classification by ensembles of deep convolutional networks and regularly spaced shifting," *IEEE Access*, vol. 9, pp. 112193–112205, 2021, doi: 10.1109/ACCESS.2021.3103410.
- [17] N. Rezaeana, M. S. Hossain, and K. Andersson, "Detection and Classification of Skin Cancer by Using a Parallel CNN Model," *Proc. 2020 IEEE Int. Women Eng. Conf. Electr. Comput. Eng. WIECON-ECE 2020*, pp. 380–386, 2020, doi: 10.1109/WIECON-ECE52138.2020.9397987.
- [18] R. Raja Subramanian, D. Achuth, P. Shiridi Kumar, K. N. Kumar Reddy, S. Amara, and A. S. Chowdary, "Skin cancer classification using Convolutional neural networks," *Proc. Conflu. 2021 11th Int. Conf. Cloud Comput. Data Sci. Eng.*, pp. 13–19, 2021, doi: 10.1109/Confluence51648.2021.9377155.
- [19] A. Ameri, "A deep learning approach to skin cancer detection in dermoscopy images," *J. Biomed. Phys. Eng.*, vol. 10, no. 6, pp. 801–806, 2020, doi: 10.31661/jbpe.v0i0.2004-1107.
- [20] M. F. Jojoa Acosta, L. Y. Caballero Tovar, M. B. Garcia-Zapirain, and W. S. Percybrooks, "Melanoma diagnosis using deep learning techniques on dermatoscopic images," *BMC Med. Imaging*, vol. 21, no. 1, pp. 1–11, 2021, doi: 10.1186/s12880-020-00534-8.
- [21] P. Shan, Y. Wang, C. Fu, W. Song, and J. Chen, "Automatic skin lesion segmentation based on FC-DPN,"

- Comput. Biol. Med.*, vol. 123, no. March, p. 103762, 2020, doi: 10.1016/j.compbimed.2020.103762.
- [22] A. A. Adegun and S. Viriri, "Deep learning-based system for automatic melanoma detection," *IEEE Access*, vol. 8, pp. 7160–7172, 2020, doi: 10.1109/ACCESS.2019.2962812.
- [23] L. Zhang, G. Yang, and X. Ye, "Automatic skin lesion segmentation by coupling deep fully convolutional networks and shallow network with textons," *J. Med. Imaging*, vol. 6, no. 02, p. 1, 2019, doi: 10.1117/1.jmi.6.2.024001.
- [24] L. Bi, J. Kim, E. Ahn, A. Kumar, D. Feng, and M. Fulham, "Step-wise integration of deep class-specific learning for dermoscopic image segmentation," *Pattern Recognit.*, vol. 85, pp. 78–89, 2019, doi: 10.1016/j.patcog.2018.08.001.
- [25] M. Nawaz *et al.*, "Skin cancer detection from dermoscopic images using deep learning and fuzzy k-means clustering," *Microsc. Res. Tech.*, vol. 85, no. 1, pp. 339–351, 2022, doi: 10.1002/jemt.23908.
- [26] M. Nawaz *et al.*, "Melanoma localization and classification through faster region-based convolutional neural network and SVM," *Multimed. Tools Appl.*, vol. 80, no. 19, pp. 28953–28974, 2021, doi: 10.1007/s11042-021-11120-7.
- [27] I. Iqbal, M. Younus, K. Walayat, M. U. Kakar, and J. Ma, "Automated multi-class classification of skin lesions through deep convolutional neural network with dermoscopic images," *Comput. Med. Imaging Graph.*, vol. 88, no. January 2023, 2021, doi: 10.1016/j.compmedimag.2020.101843.
- [28] S. Banerjee, S. K. Singh, A. Chakraborty, A. Das, and R. Bag, "Melanoma Diagnosis Using Deep Learning and Fuzzy Logic," *Diagnostics*, vol. 10, p. 577, 2020, [Online]. Available: doi:10.3390/diagnostics10080577.
- [29] M. A. Riyadi, A. Ayuningtias, and R. R. Isnanto, "Detection and Classification of Skin Cancer Using YOLOv8n," in *2024 11th International Conference on Electrical Engineering, Computer Science and Informatics (EECSI)*, Sep. 2024, pp. 9–15, doi: 10.1109/EECSI63442.2024.10776505.
- [30] P. Rajeshkumar, S. Kharche, P. Poojari, S. Utekar, S. Saini, and S. Bidwai, "DermAI: An Innovative AI-Driven Chatbot for Enhanced Dermatological Diagnosis and Patient Interaction," *Indones. J. Electr. Eng. Informatics*, vol. 12, no. 4, Dec. 2024, doi: 10.52549/ijeei.v12i4.5806.
- [31] M. A. Khan, T. Akram, Y. D. Zhang, and M. Sharif, "Attributes based skin lesion detection and recognition: A mask RCNN and transfer learning-based deep learning framework," *Pattern Recognit. Lett.*, vol. 143, pp. 58–66, 2021, doi: 10.1016/j.patrec.2020.12.015.
- [32] R. Kaur, H. Gholamhosseini, R. Sinha, and M. Lindén, "Melanoma Classification Using a Novel Deep Convolutional Neural Network with Dermoscopic Images," *Sensors*, vol. 22, no. 3, pp. 1–15, 2022, doi: 10.3390/s22031134.
- [33] O. O. Abayomi-Alli, R. Damaševičius, S. Misra, R. Maskeliūnas, and A. Abayomi-Alli, "Malignant skin melanoma detection using image augmentation by oversampling in nonlinear lower-dimensional embedding manifold," *Turkish J. Electr. Eng. Comput. Sci.*, vol. 29, pp. 2600–2614, 2021, doi: 10.3906/elk-2101-133.
- [34] J. Jiang, J. Guo, M. Khan, Y. Cui, and W. Lin, "Energy-saving Service Offloading for the Internet of Medical Things Using Deep Reinforcement Learning," *ACM Trans. Sens. Networks*, vol. 19, no. 3, Mar. 2023, doi: 10.1145/3560265.
- [35] K. Hameed Abdulkareem *et al.*, "Smart Healthcare System for Severity Prediction and Critical Tasks Management of COVID-19 Patients in IoT-Fog Computing Environments," *Comput. Intell. Neurosci.*, vol. 2022, no. July, 2022, doi: 10.1155/2022/5012962.
- [36] B. C. R. S. Furriel *et al.*, "Artificial intelligence for skin cancer detection and classification for clinical environment: a systematic review," *Front. Med.*, vol. 10, Jan. 2024, doi: 10.3389/fmed.2023.1305954.
- [37] B. Cassidy, C. Kendrick, A. Brodzicki, J. Jaworek-Korjakowska, and M. H. Yap, "Analysis of the ISIC image datasets: Usage, benchmarks and recommendations," *Med. Image Anal.*, vol. 75, p. 102305, 2022, doi: 10.1016/j.media.2021.102305.
- [38] P. Tschandl, C. Rosendahl, and H. Kittler, "Data descriptor: The HAM10000 dataset, a large collection of multi-source dermatoscopic images of common pigmented skin lesions," *Sci. Data*, vol. 5, Aug. 2018, doi: 10.1038/sdata.2018.161.
- [39] N. C. F. Codella *et al.*, "Skin lesion analysis toward melanoma detection: A challenge at the 2017 International symposium on biomedical imaging (ISBI), hosted by the international skin imaging collaboration (ISIC)," *Proc. - Int. Symp. Biomed. Imaging*, vol. 2018-April, pp. 168–172, 2018, doi: 10.1109/ISBI.2018.8363547.
- [40] "DermIS." <https://www.dermis.net/dermisroot/en/home/index.htm> (accessed Jun. 28, 2024).
- [41] I. Giotis, N. Molders, S. Land, M. Biehl, M. F. Jonkman, and N. Petkov, "MED-NODE: A computer-assisted melanoma diagnosis system using non-dermoscopic images," *Expert Syst. Appl.*, vol. 42, no. 19, pp. 6578–6585, Nov. 2015, doi: 10.1016/j.eswa.2015.04.034.
- [42] T. Mendonca, P. M. Ferreira, J. S. Marques, A. R. S. Marcal, and J. Rozeira, "PH2 - A dermoscopic image database for research and benchmarking," in *2013 35th Annual International Conference of the IEEE Engineering in Medicine and Biology Society (EMBC)*, Jul. 2013, pp. 5437–5440, doi: 10.1109/EMBC.2013.6610779.
- [43] D. Gutman *et al.*, "Skin Lesion Analysis toward Melanoma Detection: A Challenge at the International Symposium on Biomedical Imaging (ISBI) 2016, hosted by the International Skin Imaging Collaboration (ISIC)," pp. 3–7, 2016, [Online]. Available: <http://arxiv.org/abs/1605.01397>.
- [44] M. Combalia *et al.*, "BCN20000: Dermoscopic Lesions in the Wild," 2019, doi: 10.1038/s41597-024-03387-w.
- [45] J. Wang *et al.*, "Generalizing to Unseen Domains: A Survey on Domain Generalization," *IEEE Trans. Knowl. Data Eng.*, pp. 1–1, 2022, doi: 10.1109/TKDE.2022.3178128.

- [46] Z. Hussain, F. Gimenez, D. Yi, and D. Rubin, "Differential Data Augmentation Techniques for Medical Imaging Classification Tasks," *AMIA ... Annu. Symp. proceedings. AMIA Symp.*, vol. 2017, pp. 979–984, 2017.
- [47] I. Tougui, A. Jilbab, and J. El Mhamdi, "Impact of the Choice of Cross-Validation Techniques on the Results of Machine Learning-Based Diagnostic Applications," *Healthc. Inform. Res.*, vol. 27, no. 3, pp. 189–199, Jul. 2021, doi: 10.4258/hir.2021.27.3.189.
- [48] J. Kaliappan, A. R. Bagepalli, S. Almal, R. Mishra, Y.-C. Hu, and K. Srinivasan, "Impact of Cross-Validation on Machine Learning Models for Early Detection of Intrauterine Fetal Demise," *Diagnostics*, vol. 13, no. 10, p. 1692, May 2023, doi: 10.3390/diagnostics13101692.
- [49] D. Berrar, "Cross-Validation," in *Encyclopedia of Bioinformatics and Computational Biology*, Elsevier, 2019, pp. 542–545.
- [50] K. Matsunaga, A. Hamada, A. Minagawa, and H. Koga, "Image Classification of Melanoma, Nevus and Seborrheic Keratosis by Deep Neural Network Ensemble," pp. 2–5, 2017, [Online]. Available: <http://arxiv.org/abs/1703.03108>.
- [51] I. Gonzalez-Diaz, "DermaKNet: Incorporating the Knowledge of Dermatologists to Convolutional Neural Networks for Skin Lesion Diagnosis," *IEEE J. Biomed. Heal. Informatics*, vol. 23, no. 2, pp. 547–559, Mar. 2019, doi: 10.1109/JBHI.2018.2806962.
- [52] A. Menegola, J. Tavares, M. Fornaciali, L. T. Li, S. Avila, and E. Valle, "RECOD Titans at ISIC Challenge 2017," no. March, 2017, [Online]. Available: <http://arxiv.org/abs/1703.04819>.
- [53] A. Menegola, M. Fornaciali, R. Pires, F. V. Bittencourt, S. Avila, and E. Valle, "Knowledge transfer for melanoma screening with deep learning," *Proc. - Int. Symp. Biomed. Imaging*, pp. 297–300, 2017, doi: 10.1109/ISBI.2017.7950523.
- [54] Y. Jusman, I. M. Firdiantika, D. A. Dharmawan, and K. Purwanto, "Performance of Multi Layer Perceptron and Deep Neural Networks in Skin Cancer Classification," in *2021 IEEE 3rd Global Conference on Life Sciences and Technologies (LifeTech)*, Mar. 2021, pp. 534–538, doi: 10.1109/LifeTech52111.2021.9391876.
- [55] M. Vilares Ferro, Y. Doval Mosquera, F. J. Ribadas Pena, and V. M. Darriba Bilbao, "Early stopping by correlating online indicators in neural networks," *Neural Networks*, vol. 159, pp. 109–124, Feb. 2023, doi: 10.1016/j.neunet.2022.11.035.
- [56] Y. Bai *et al.*, "Understanding and Improving Early Stopping for Learning with Noisy Labels," *Adv. Neural Inf. Process. Syst.*, vol. 29, no. NeurIPS, pp. 24392–24403, 2021.
- [57] N. Srivastava, G. Hinton, A. Krizhevsky, I. Sutskever, and R. Salakhutdinov, "Dropout: A simple way to prevent neural networks from overfitting," *J. Mach. Learn. Res.*, vol. 15, pp. 1929–1958, 2014.
- [58] J. Tompson, R. Goroshin, A. Jain, Y. LeCun, and C. Bregler, "Efficient object localization using Convolutional Networks," in *2015 IEEE Conference on Computer Vision and Pattern Recognition (CVPR)*, Jun. 2015, pp. 648–656, doi: 10.1109/CVPR.2015.7298664.
- [59] T. Zhou, X. Ye, H. Lu, X. Zheng, S. Qiu, and Y. Liu, "Dense Convolutional Network and Its Application in Medical Image Analysis," *Biomed Res. Int.*, vol. 2022, pp. 1–22, Apr. 2022, doi: 10.1155/2022/2384830.
- [60] G. Huang, Z. Liu, L. Van Der Maaten, and K. Q. Weinberger, "Densely Connected Convolutional Networks," in *2017 IEEE Conference on Computer Vision and Pattern Recognition (CVPR)*, Jul. 2017, pp. 2261–2269, doi: 10.1109/CVPR.2017.243.
- [61] M. Dildar *et al.*, "Skin Cancer Detection: A Review Using Deep Learning Techniques," *Int. J. Environ. Res. Public Health*, vol. 18, no. 10, p. 5479, May 2021, doi: 10.3390/ijerph18105479.
- [62] S. Moldovanu, C.-D. Obreja, K. C. Biswas, and L. Moraru, "Towards Accurate Diagnosis of Skin Lesions Using Feedforward Back Propagation Neural Networks," *Diagnostics*, vol. 11, no. 6, p. 936, May 2021, doi: 10.3390/diagnostics11060936.
- [63] L. Alzubaidi *et al.*, *Review of deep learning: concepts, CNN architectures, challenges, applications, future directions*, vol. 8, no. 1. Springer International Publishing, 2021.
- [64] S. R D and S. A, "Deep Learning Based Skin Lesion Segmentation and Classification of Melanoma Using Support Vector Machine (SVM)," *Asian Pacific J. Cancer Prev.*, vol. 20, no. 5, pp. 1555–1561, May 2019, doi: 10.31557/APJCP.2019.20.5.1555.
- [65] D. Keerthana, V. Venugopal, M. K. Nath, and M. Mishra, "Hybrid convolutional neural networks with SVM classifier for classification of skin cancer," *Biomed. Eng. Adv.*, vol. 5, p. 100069, Jun. 2023, doi: 10.1016/j.bea.2022.100069.
- [66] P. Banasode, M. Patil, and N. Ammanagi, "A Melanoma Skin Cancer Detection Using Machine Learning Technique: Support Vector Machine," *IOP Conf. Ser. Mater. Sci. Eng.*, vol. 1065, no. 1, p. 012039, Feb. 2021, doi: 10.1088/1757-899X/1065/1/012039.
- [67] J. B. A. Das, D. Mishra, A. Das, M. N. Mohanty, and A. Sarangi, "Skin cancer detection using machine learning techniques with ABCD features," in *2022 2nd Odisha International Conference on Electrical Power Engineering, Communication and Computing Technology (ODICON)*, Nov. 2022, pp. 1–6, doi: 10.1109/ODICON54453.2022.10009956.
- [68] M. Q. Hatem, "Skin lesion classification system using a K-nearest neighbor algorithm," *Vis. Comput. Ind. Biomed. Art*, vol. 5, no. 1, p. 7, Dec. 2022, doi: 10.1186/s42492-022-00103-6.
- [69] K. Vikas Reddy and L. Rama Parvathy, "Accurate Detection and Classification of Melanoma Skin Cancer Using Decision Tree Algorithm over CNN," 2022.
- [70] A. Shah *et al.*, "A comprehensive study on skin cancer detection using artificial neural network (ANN) and convolutional neural network (CNN)," *Clin. eHealth*, vol. 6, pp. 76–84, Dec. 2023, doi: 10.1016/j.ceh.2023.08.002.

- [71] H. K. Kondaveeti and P. Edupuganti, "Skin Cancer Classification using Transfer Learning," in *2020 IEEE International Conference on Advent Trends in Multidisciplinary Research and Innovation (ICATMRI)*, Dec. 2020, pp. 1–4, doi: 10.1109/ICATMRI51801.2020.9398388.
- [72] R. Maiti, P. Agarwal, R. R. Kumar, and A. Bhat, "Detection Of Skin Cancer Using Neural Architecture Search with Model Quantization," in *2021 5th International Conference on Intelligent Computing and Control Systems (ICICCS)*, May 2021, pp. 1807–1814, doi: 10.1109/ICICCS51141.2021.9432190.
- [73] R. Rokhana, W. Herulambang, and R. Indraswari, "Deep Convolutional Neural Network for Melanoma Image Classification," in *2020 International Electronics Symposium (IES)*, Sep. 2020, pp. 481–486, doi: 10.1109/IES50839.2020.9231676.
- [74] H. Huang, B. W. Hsu, C. Lee, and V. S. Tseng, "Development of a light-weight deep learning model for cloud applications and remote diagnosis of skin cancers," *J. Dermatol.*, vol. 48, no. 3, pp. 310–316, Mar. 2021, doi: 10.1111/1346-8138.15683.
- [75] S. S. Chaturvedi, J. V. Tembume, and T. Diwan, "A multi-class skin Cancer classification using deep convolutional neural networks," *Multimed. Tools Appl.*, vol. 79, no. 39–40, pp. 28477–28498, Oct. 2020, doi: 10.1007/s11042-020-09388-2.

## BIOGRAPHY OF AUTHORS



Kavita Behara is a Senior Lecturer in the Department of Electrical Engineering at the Mangosuthu University of Technology, where she coordinates Computer Engineering. She is a Ph.D. candidate in the Discipline of Electrical, Electronics, and Computer Engineering at the University of KwaZulu-Natal, South Africa. She received her M.Sc. degree in computer science from Andhra University, India, in 2001. She has over 20 years of experience in teaching and managing academic programmes in higher education. Kavita is a certified IBM specialist for Application Security and Networks. Her research focuses on the application of AI. She worked on robotic projects with organizations (e.g., UKZN, Lego Robotics). She has participated as a keynote speaker in various conferences. Currently, her focus is on developing skin cancer detection systems using computer vision and image processing. She has memberships with IEEE, IITPSA, and INCOSE. In 2020, she won the Vice-Chancellors award for Excellence in T&L.



Ernest Bhero is an electronic engineer by profession. He is also an advocate of the High Court of South Africa. He has worked as a chief design engineer for at least 4 years and has university lecturing experience spanning over 10 years. Both his honors and master's degree projects were implemented in the industry. He is a hands-on person. He designed and developed at least four different electronic products that were commercialized in his country of birth. Recently, he designed and developed an electronic system, which is being tested in the industry by a company in South Africa. He has a deep interest not only in finding practical engineering solutions to engineering problems but also in relevant IP law.



Prof Agee obtained his first degree in 1989 from the Abubakar Tafawa Balewa University (ATBU), Bauchi, Nigeria. After a year of National Service, Agee began his academic career at the ATBU as a Graduate Assistant in September 1990, where he Lectured until 2003. During his period at the ATBU, he rose to become a Senior Lecturer in 2001; and also obtained a Master's degree (1992), a PhD (2000) at the ATBU, and also undertook a Postdoctoral Programme at the Ecoles des Mines de Paris, France. His further academic appointments include a Lecturer position at the University of Botswana (Jan. 2004-Dec. 2009); Associate of Professor of Control and Process Control at the Tshwane University of Technology, Pretoria (Dec. 2009-June 2015); and his current position at the University of KwaZulu Natal, where he has been since July 2015.